Journal of Cosmology and Astroparticle Physics
An IOP and SISSA journal

Received: *September 26, 2025*
Revised: *December 2, 2025*
Accepted: *February 9, 2026*
Published: *April 10, 2026*

The simple way to measure evolving dark energy without prior-volume effects

Maria Tsedrik[a,b], **Pedro Carrilho**[c,a] **and Chiara Moretti**[d,e,f]

[a] *Institute for Astronomy, The University of Edinburgh, Royal Observatory, Edinburgh EH9 3HJ, U.K.*
[b] *Higgs Centre for Theoretical Physics, School of Physics and Astronomy, The University of Edinburgh, Mayfield Road, Edinburgh EH9 3JZ, U.K.*
[c] *Centre for Astrophysics Research, University of Hertfordshire, College Lane, Hatfield AL10 9AB, U.K.*
[d] *INAF, Osservatorio Astronomico di Trieste, Via Tiepolo 11, 34143 Trieste, Italy*
[e] *Institute for Fundamental Physics of the Universe, Via Beirut 2, 34151 Trieste, Italy*
[f] *Istituto Nazionale di Fisica Nucleare, Sezione di Trieste, via Valerio 2, 34127 Trieste, Italy*

E-mail: mtsedrik@ed.ac.uk, p.carrilho@herts.ac.uk, chiara.moretti@inaf.it

Abstract: We present a simple yet effective method to resolve prior-volume effects, also known as projection effects, in full-shape analyses of the power spectrum multipoles within the Effective Field Theory of Large-Scale Structure (EFTofLSS). By re-defining the EFTofLSS nuisance parameters to incorporate the contribution from the parameters impacting the amplitude of the EFTofLSS modelling components, we substantially mitigate projection effects. With the re-parametrisation the actual posterior maximum values are within the marginalised credible interval, eliminating significant shifts observed in the baseline analysis. We demonstrate the robustness of this method in full-shape w_0w_aCDM analyses on synthetic data in BOSS DR12 and DESI DR1 setups. We find that the re-parametrisation with the Alcock-Paczynski amplitude is important for unbiased constraints in dark energy models beyond Λ. For the evolving dark energy model, we then analyse the BOSS DR12 measurements, in combination with BAO information (from BOSS DR12, 6DF, SDSS DR7 MGS and eBOSS DR16 surveys) and $3 \times 2\,\mathrm{pt}$ measurements from DES Y3 — all data combinations are converging into the $w_0 - w_a$ parameter region preferred by DESI+CMB+SNIa. From total combination of these large-scale structure probes without additional CMB information we find $w_0 = -0.72 \pm 0.21$, $w_a = -0.91^{+0.78}_{-0.64}$. Despite the low significance of deviation from

https://doi.org/10.1088/1475-7516/2026/04/030

JCAP04(2026)030

standard cosmology, this result underscores the potential of our re-parametrisation approach in delivering low-redshift cosmological constraints. We argue for the use of this approach in spectroscopic Stage IV surveys, where the potential deviation from standard cosmology can be detected with higher significance.

Keywords: Bayesian reasoning, cosmological parameters from LSS, dark energy theory

ArXiv ePrint: 2509.09562

JCAP04(2026)030

Contents

1 Introduction

Spectroscopic surveys of Large-Scale Structure (LSS), such as the Baryon Oscillation Spectroscopic Survey (BOSS) [1], its extension eBOSS [2], and recently the Dark Energy Spectroscopic Instrument (DESI), [3] measured redshifts of millions of galaxies. These measurements can be translated into spatial distribution of galaxies, from which we can learn key cosmological information. From a "bump", an excess of signal in the two-point correlation function of these galaxies measured at different redshifts, we can measure cosmological expansion and matter density [4, 5]. Such excess of signal is known as baryonic acoustic oscillations (BAO), and can be used as a standard ruler: its position encodes the size of the Universe at the epoch slightly after re-combination. Beyond this feature, we can explore the shape of two-point correlators in redshift space and their Fourier-transform, the power spectrum multipoles. From these we can gain additional information on the growth of cosmic structures, the amplitude and shape of the primordial power spectrum [6, 7].

While in principle containing more cosmological information than BAO, a full-shape (FS) analysis also demands a more complex modelling prescription. Currently, the standard theoretical framework for modelling power spectrum multipoles in a FS analysis is the effective field theory of large-scale structure (EFTofLSS) [8–13]. The EFTofLSS approach allows us to model the power spectrum multipoles in redshift space up to mildly nonlinear scales. Based on standard perturbation theory of structure formation, it includes contributions from smaller astrophysical scales via a small number of additional parameters, the so-called counterterms. In addition to the counterterms, the model includes other nuisance parameters such as those

JCAP04(2026)030

related to galaxy bias and shot noise contributions. Although these parameters allow the EFTofLSS to successfully fit a broad range of cosmologies (e.g., modified gravity [14, 15], dark energy models [16, 17], various galaxy-halo connections [18]), they also introduce projection or prior-volume effects, which complicate the interpretation of cosmological inferences. Projection effects arise when a high-dimensional non-Gaussian posterior distribution is compressed in a lower-dimensional parameter space [19, 20]. They are manifested by the best-fit, i.e. the Maximum *A Posteriori* (MAP) value being in disagreement with the peak of the marginalised posterior [21, 22]. This disagreement appears when unconstrained or weakly constrained regions of the nuisance parameter space significantly contribute to the marginalised posterior of cosmological parameters. Projection effects within EFTofLSS are especially prominent for beyond-ΛCDM cosmologies, in which additional parameters are strongly degenerate with cosmological and nuisance parameters [23, 24]. Potential solutions to mitigate projection effects include various methods, such as informative priors on cosmological parameters motivated by CMB measurements [19, 23]; Jeffreys priors [25] on nuisance parameters [26–28]; priors on nuisance parameters informed by halo occupation distributions [29, 30]; combination with external probes [31].

In this work we propose a simple solution — a re-parametrisation scheme[1] for the nuisance parameters of the EFTofLSS. A similar approach is presented in the baseline analysis of DESI DR1 [24, 32], its re-analysis [33, 34], and photometric clustering with perturbative galaxy bias with DES Y3 [35, 36]. There, the nuisance parameters absorb σ_8, a parameter that corresponds to the normalisation of the power spectrum defined as the variance of the density field smoothed within a radius $R = 8\,\mathrm{Mpc}\,h^{-1}$. Such re-parametrisation helps connecting the model parameters with the observed power spectrum multipoles (or angular correlation functions in case of DES) and reducing biases from projection effects. Following the same logic, we propose that absorbing the Alcock-Paczynski (AP) [37] amplitude significantly reduces projection effects for dark energy models beyond cosmological constant in FS analysis. The AP effect introduces anisotropies in the measured multipoles because of a discrepancy between the fiducial cosmology, assumed to convert redshifts to distances, and the true underlying cosmology. It also re-scales the overall amplitude of the signal.

This paper combines two topics: (1) mitigating projection effects via re-parametrisation of the EFTofLSS parameters and (2) constraining evolving dark energy with Stage III (pre-DESI) LSS data. The first topic is covered in sections 3 and 4. There, we discuss prior-volume effects in FS analysis (section 3). We also study various re-parametrisations of the EFTofLSS nuisance parameters in a FS analysis with synthetic Stage III data (section 4.1) and then apply the best solution to a synthetic Stage IV scenario (section 4.2). The second topic of this paper is covered in sections 2, 4.1 and 5. We specify the different sets of Stage III data and the setup used in our analysis in section 2. We provide constraints for the evolving dark energy parameters in BOSS DR12 FS analysis with our re-parametrisation in section 4.1. Then in sections 5.1–5.2, we add information from BAO (BOSS and external) and photometric probes (DES Y3) to gain more information from available LSS probes and provide constraints independent from the cosmic microwave background (CMB) and supernova (SN) measurements.

[1]For a simpler toy-example of the re-parametrisation and its impact on prior-volume effects see the corresponding discussion in section 2.3 of ref. [22].

JCAP04(2026)030

2 Data and analysis setup

We first summarise all the cosmological probes and analysis setups used in our inference. Note that, if not explicitly stated otherwise, we use the `Nautilus`-sampler [38] to explore the parameter space. Additionally, marginalised posteriors and credible intervals are obtained using `GetDist`[2] [39], while for all MAP-values of the un-marginalised posterior distribution we use a minimiser called `minuit`.[3]

BOSS. The main focus of this work is FS analysis, for it we consider the galaxy power spectrum multipoles from BOSS DR12 [40–42]. The dataset consists of two galaxy samples: CMASS and LOWZ with effective redshifts $z_1 = 0.38$ and $z_3 = 0.61$, respectively. Each sample covers two different sky cuts, NGC in the north and SGC in the south. Hence in total, we fit 4 independent sets of multipoles. The multipole measurements and covariance[4] are provided in ref. [43] and are obtained with the windowless estimator [44, 45]. The covariance is computed from "MultiDark-Patchy" mock catalogues [46, 47]. Complementarily, we also use four BAO measurements from BOSS DR12 in the same patches of sky [43] (with the corresponding cross-covariance when combined with the multipoles). Further in the text, "FS" analysis includes only the multipoles, "FS+BAO" and "BOSS" denote the analysis with the multipoles in combination with the BAO data. In terms of the analysis choices, we keep priors on cosmological parameters broad and only impose Gaussian priors on the baryon density (BBN prior [48–50]) and spectral index (10 times the standard deviation from Planck's constraints [51], similar to the DESI DR1 setup). Priors on the nuisance parameters in the baseline analysis are given in the left part of table 2. Priors on the evolving dark energy parameters are uniform: $w_0 \in [-3, -0.3]$, $w_a \in [-3, 3]$, and with the following condition for the matter-domination epoch: $w_0 + w_a < 0$. We fit the power spectrum multipoles (P_0, P_2, P_4) with the identical scale-cuts of $k_{\rm max} = 0.2\,h/{\rm Mpc}$. Our analysis setup and likelihood pipeline are discussed in detail in refs. [19, 23].

Synthetic data (Stage III). To study projection effects in section 4.1, we create synthetic noiseless data vectors of BOSS-like power spectrum multipoles. The goal of our study is to understand the shifts between maxima of the unmarginalised and marginalised posterior distributions driven exclusively by prior-volume effects from the EFTofLSS nuisance parameters. With noisy synthetic data, the posterior peaks can be shifted within 1σ of the fiducial parameters due to statistical fluctuations even in the absence of any prior-volume effects. To avoid such additional uncertainty we work with noiseless synthetic data. In the synthetic data analysis we use the same covariance as in the BOSS DR12 real data analysis. For fiducial cosmological parameters we take $\omega_{\rm c} = 0.12$, $\omega_{\rm b} = 0.02268$, $h = 0.68$, $n_{\rm s} = 0.97$, $\ln(10^{10} A_{\rm s}) = 3.044$, $w_0 = -1$, $w_a = 0$, $M_\nu = 0.06\,{\rm eV}$, while the nuisance parameters are determined by maximising the full likelihood with cosmology fixed to the fiducial values. In figure 1 we show the agreement in the baseline FS analysis for evolving dark energy on real data (blue) and synthetic ΛCDM data (orange). With noiseless synthetic data we also demonstrate that all cosmological parameters recover their true values in the baseline analysis when all

[2] https://github.com/cmbant/getdist
[3] https://github.com/jpivarski/pyminuit
[4] https://github.com/oliverphilcox/full_shape_likelihoods/tree/main/data

JCAP04(2026)030

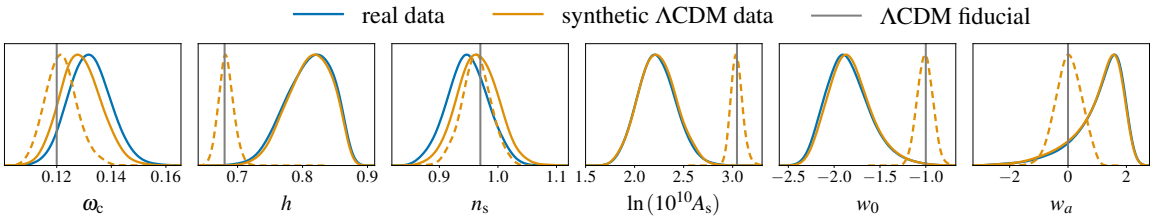

Figure 1. Baseline FS analysis: 1D marginalised constraints on cosmological parameters on real BOSS DR12 data (blue) and synthetic ΛCDM data (orange). Solid lines denote the baseline analysis with all parameters varied, while the dashed lines denote the baseline analysis with nuisance parameters fixed to their fiducial values. Fiducial values of cosmological parameters in the synthetic data are shown by the grey lines.

Galaxy sample	$z_{\rm eff}$	V_s [Gpc$^3/h^3$]	b_1	$\bar{n}$ [h^3/Mpc^3]
BGS	0.2	0.94	1.14	3.2×10^{-4}
LRGs	0.8	7.88	2.56	2.7×10^{-4}
ELG	1.2	14.32	1.51	1.7×10^{-4}

Table 1. Parameters used to generate the synthetic DESI-like data-vectors in DR1 scenario. We follow ref. [3] in computing the effective redshift $z_{\rm eff}$ and determining the linear bias b_1. Total volume and number density is computed with numbers from ref. [52].

nuisance parameters are fixed to their fiducial values. As expected, when cosmological and nuisance parameters are varied in the baseline analysis, we observe shifts towards lower A_s values, which are present in the analyses of standard and extended cosmologies (see refs. [19, 23, 31]). We also observe shifts due to additional degeneracy between the evolving dark energy and expansion rate parameters: h is shifted towards the upper prior bound, while the dark energy parameters prefer $w_0 < -1$ and $w_a > 0$. The driving mechanisms for both cases is discussed in the following section 4.

Synthetic data (Stage IV). To demonstrate robustness of our re-parametrisation approach in section 4.2, we create synthetic noiseless data vectors of DESI DR1-like power spectrum multipoles. We follow the steps described in section 4.3 of ref. [23]: we assume the same fiducial values for the cosmological parameters as above and simulating the three galaxy samples that are the target of DESI. This is repeated in two scenarios: standard cosmology ($w_0 = -1$, $w_a = 0$) and evolving dark energy ($w_0 = -0.42$, $w_a = -1.75$). Values of effective redshifts and linear galaxy bias are taken from ref. [3], while number density of the samples and their total volume are computed with numbers from table 2 of ref. [52]. We list these numbers in table 1. For the analysis we use the analytical covariance computed following ref. [53] and scale-cuts of $k_{\rm max} = 0.25\,h$/Mpc for all multipoles.

extBAO. In section 5, we combine BOSS DR12 measurements with external BAO, namely with pre-reconstruction BAO measurements at low redshift from the 6DF survey [54] and SDSS DR7 MGS [55]. We also add information from high redshift measurements of the

JCAP04(2026)030

Hubble factor and angular diameter distance from the Ly-α forest auto and cross-correlation with quasars from eBOSS DR16 [56].

DESY3. In section 5, we also add $3\times2\,$pt correlation functions from DES Y3 [57, 58]. They contain cosmic shear, galaxy clustering and galaxy-galaxy lensing information from sources in four redshift-bins and lenses from the first four redshift-bins of the MagLim sample [59]. The corresponding covariance matrix is obtained analytically as described and validated in ref. [60]. We use the same scale-cuts as in the DES Y3 ΛCDM baseline analysis [61] and model the nonlinear power spectrum with `HMcode2020` [62]. We use the official DES-pipeline, `CosmoSIS`,[5] in which we substitute the computation of linear and nonlinear matter power spectra with an emulator, `HMcode2020-emulator`,[6] trained with `cosmopower`[7] [63]. We use the pipeline developed for the joint spectroscopic and photometric analysis from ref. [31].

Planck+DESI+DESY5SN. Finally, we repeat DESI DR2 BAO analysis [64] in combination with the CMB (Planck 2018 low-ℓ TT and EE, CamSpec TT/TE/EE, and PR4 lensing [65]) and DES Y5 SN [66] using publicly available likelihoods in `Cobaya`.[8] The constraints we obtain are in good agreement with the official DESI results from ref. [64]. The purpose of repeating this analysis is to plot the corresponding posteriors for the evolving dark energy parameters together with the results of our Stage III LSS-only analysis in figure 8.

3 Prior-volume effects in full-shape analysis

In our modelling of the power spectrum multipoles we follow a prescription analogous to the one of ref. [67], but employ the independent implementation in the `PBJ` code. The latter has been extensively validated on N-body simulations in ΛCDM [68–72]. Below we outline the key components relevant for the discussion on projection effects, but refer to refs. [19, 23] for a more detailed description. The one-loop EFTofLSS galaxy power spectrum at a fixed redshift can be written as

$$P_{\rm gg}(k,\mu) = P_{\rm SPT}(\boldsymbol{k}) + P_{\rm ctr}(\boldsymbol{k}) + P_{\rm stoch}(\boldsymbol{k})\,. \tag{3.1}$$

The first term is a standard perturbation theory one-loop power spectrum with the redshift space kernels from ref. [73] and integrals of the linear power spectrum, $P_{\rm L}$, with various powers and combinations of galaxy bias parameters — b_1, b_2, $b_{\mathcal{G}_2}$, b_{Γ_3} [74, 75]. The term important for our discussion is

$$P_{b_{\Gamma_3}}(k,\mu) = b_{\Gamma_3}(b_1 + f\mu^2)P_{13}(k,\mu)\,, \tag{3.2}$$

where P_{13} is a loop-correction integral proportional to $P_{\rm L}^2$, μ is the cosine of the angle between the wavevector $\boldsymbol{k}$ and the line of sight, f is the growth rate. The second term from eq. (3.1) is the EFTofLSS counterterm contribution:

$$\begin{aligned} P_{\rm ctr}(k,\mu) = &-2\tilde{c}_0 k^2 P_{\rm L}(k) - 2\tilde{c}_2 k^2 f\mu^2 P_{\rm L}(k) - 2\tilde{c}_4 k^2 f^2\mu^4 P_{\rm L}(k) \\ &+ c_{\nabla^4\delta} k^4 f^4\mu^4 (b_1 + f\mu^2)^2 P_{\rm L}(k)\,. \end{aligned} \tag{3.3}$$

[5] https://github.com/joezuntz/cosmosis-standard-library
[6] https://github.com/MariaTsedrik/HMcode2020Emu
[7] https://github.com/alessiospuriomancini/cosmopower
[8] https://github.com/CobayaSampler/cobaya

JCAP04(2026)030

Following ref. [67], we re-define the k^2-counterterm parameters ($\tilde{c}_0$, $\tilde{c}_2$, $\tilde{c}_4$) in order to have separate contributions to each multipole. Lastly, the third term from eq. (3.1) contains the shot-noise contribution:

$$P_{\rm stoch}(k,\mu) = N + e_0 k^2 + e_2 k^2 \mu^2 \,, \tag{3.4}$$

where N is a constant that includes deviations from pure Poisson shot noise, and we have two additional scale-dependent terms with e_0 and e_2 in units of $(\mathrm{Mpc}\,h^{-1})^2$. We include the impact of the fiducial cosmology assumed when converting redshifts to distances in the data by correcting (k,μ) with AP distortions and re-scale $P_{\rm gg}$ with the AP amplitude [37]. The AP amplitude, $A_{\rm AP}$ is a function of redshift and background cosmology:

$$A_{\rm AP}(z) = \left(\frac{H_0^{\rm fid}}{H_0}\right)^3 \frac{H(z)}{H^{\rm fid}(z)} \left(\frac{D_A^{\rm fid}(z)}{D_A(z)}\right)^2 \tag{3.5}$$

with H_0 being the Hubble factor today, D_A the angular diameter distance, and the superscript $^{\rm fid}$ referring to quantities evaluated in the fiducial cosmology. Finally, we project the anisotropic power spectrum to multipoles, $P_l(k)$, with Legendre polynomials.

To accelerate the convergence of MCMC chains, we perform analytical marginalisation of nuisance parameters that appear linearly in the model (counterterms, shot-noise and the third order bias parameter) [12, 16]. We separate the power spectrum multipoles into analytically non-marginalised (nm) and marginalised (m) parts:

$$P_l(k) = P_l^{\rm nm}(k) + \sum_i n_i^{\rm m} P_{i,l}^{\rm m}(k) \,, \tag{3.6}$$

where the nuisance parameters with superscript "m" appear linearly in the model and have Gaussian priors. For a Gaussian likelihood this allows us to solve the posterior integral over $n_i^{\rm m}$ analytically. The resulting marginalised log-posterior is a function of cosmological and non-marginalised nuisance parameters $(\Omega, n^{\rm nm})$ and proportional to

$$\chi^2_{\rm m}(\Omega, n^{\rm nm}) = \chi^2_*(\Omega, n^{\rm nm}) + \ln\det F_2(\Omega, n^{\rm nm}) + \text{const.} \tag{3.7}$$

The first term on the r.h.s. is what we call the "profile likelihood", while the second term is called the Laplace term (see ref. [22] for details). They are given by

$$\chi^2_* = F_0 - F_{1,i} F^{-1}_{2,ij} F_{1,j} \,, \tag{3.8}$$

$$F_0 = \Delta_l \mathrm{Cov}^{-1}_{ll'} \Delta_{l'} + \mu_i \mathrm{C}^{-1}_{ij} \mu_j \,, \tag{3.9}$$

$$F_{1,i} = -P^{\rm m}_{i,l} \mathrm{Cov}^{-1}_{ll'} \Delta_{l'} + \mathrm{C}^{-1}_{ij} \mu_j \,, \tag{3.10}$$

$$F_{2,ij} = P^{\rm m}_{i,l} \mathrm{Cov}^{-1}_{ll'} P^{\rm m}_{j,l'} + \mathrm{C}^{-1}_{ij} \tag{3.11}$$

with $\Delta_l(k) = P_l^{\rm nm}(k) - D_l(k)$ being the difference of the non-marginalised part of the theoretical prediction with respect to the data, Cov being the covariance matrix for the data, and C_{ij} being the covariance for any possible Gaussian priors on nuisance parameters, with means μ_i. For flat priors on nuisance parameters $\mathrm{C}^{-1}_{ij} = 0$. The Laplace term is responsible for the prior-volume effects: the volume in the nuisance parameter space when integrated

JCAP04(2026)030

over fixed $(\Omega, n^{\rm nm})$. In other words, this term corresponds to the shift in the maximum of the marginalised distribution with respect to the maximum of the full distribution, because the process of marginalisation favours regions of parameter space that cover a larger volume of the probability density in the direction of integration. Improving the measurements (i.e. shrinking the covariance), or imposing informative priors on parameters makes the profile likelihood term larger and less sensitive to shifts due to the Laplace term. Note that applying Jeffreys priors on analytically marginalised parameters results in the cancellation of the Laplace term. In that case, instead of the Gaussian priors and C_{ij} in the analytically marginalised nuisance parameters, one applies Jeffreys priors $\propto \sqrt{|F(n_{\rm m})|}$ dependent on the Fisher information matrix, F. The Fisher matrix for these parameters is equivalent to the first term on the r.h.s. of eq. (3.11), hence leading to the total cancellation of the Laplace term in the marginalised posterior distribution. In that scenario, prior-volume effects due to the parameters appearing linearly in the model are fully mitigated.

Many of the nuisance parameters of the EFTofLSS model are degenerate with other amplitudes that depend on cosmological parameters. A clear case is that of counterterms in eq. (3.3), $P_{\rm ctr} \sim ck^2 P_{\rm L}$, with $P_{\rm L}$ scaling like $A_{\rm s}$ (or σ_8^2). In general, this can be written as $P_{\rm ctr} = \alpha f(k)$ where $f(k)$ controls only the scale dependence of the counterterm, while α accounts for its overall amplitude and in the current example can be written as $\alpha = cA_{\rm s}$. It is clear that the model and the corresponding likelihood can only depend on the combination α and therefore that is the only parameter that gets directly constrained, while c can only be measured with knowledge of the amplitude, $A_{\rm s}$. Providing a particular prior on c can therefore provide information that is not obvious from a first glance. To see this, let us look at the infinitesimal posterior probability in the case where only c and $A_{\rm s}$ are varied:

$$\mathrm{d}P = \mathrm{d}c\,\mathrm{d}A_{\rm s}\mathcal{L}(A_{\rm s}, c)\,, \tag{3.12}$$

where we assume a flat prior on both parameters. Instead of marginalising over c, let us first change variables from c to α:

$$\mathrm{d}P = \mathrm{d}\alpha\,\mathrm{d}A_{\rm s}\frac{1}{A_{\rm s}}\mathcal{L}(A_{\rm s}, \alpha) = \mathrm{d}\Delta\alpha\,\mathrm{d}A_{\rm s}\frac{1}{A_{\rm s}}\mathcal{L}_1(A_{\rm s})\mathcal{L}_2(\Delta\alpha)\,. \tag{3.13}$$

In this form, it is possible to separate the dependence on the amplitude from the dependence on $\Delta\alpha = \alpha - \alpha_*$, the difference of α with respect to its best-fit value. Marginalisation over $\Delta\alpha$ is then straightforward and will not affect the distribution of $A_{\rm s}$ further. This is the only form which allows us to make this separation and clearly identify the contributions from the likelihood, while extracting the effective prior on $A_{\rm s}$ that has been imposed by the original choice of a flat prior in terms of c. We see now more transparently that this flat prior is informative giving a prior in the form $1/A_{\rm s}$ (eq. (3.13)). This provides a preference for low values of the amplitude with which the nuisance parameter is degenerate, generating prior volume effects. It is also clear from this construction that the effect adds up with every additional free nuisance parameter that is degenerate with the same amplitude, giving rise to the large powers of $A_{\rm s}$ in the prior, which correspond to those in the Laplace term, as shown in the left panel of figure 2 (solid lines).

This argument applies more generally, affecting any other parameter that enters an amplitude that is degenerate with a nuisance parameter in this way. Another example is

JCAP04(2026)030

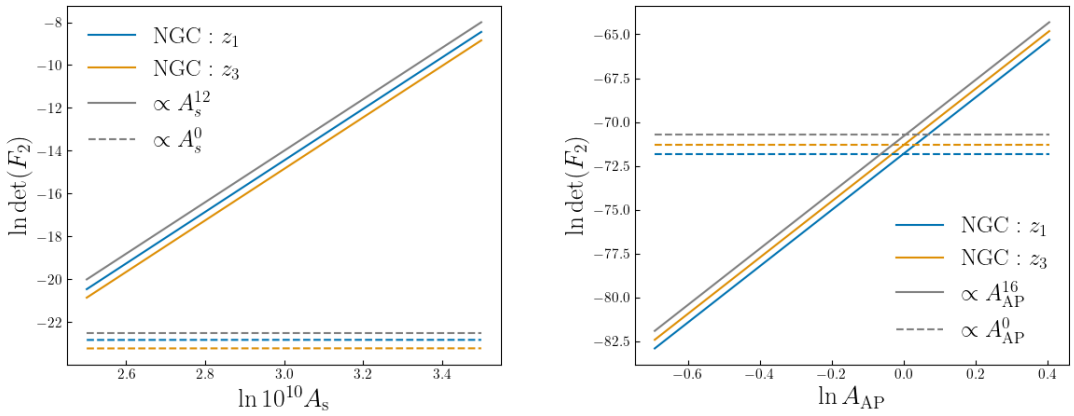

Figure 2. Illustration of the Laplace term's dependence on two amplitude-controlling parameters, primordial amplitude A_s and AP amplitude A_AP. The computation is done with the synthetic data for BOSS northern sky cuts (NGC) at two redshifts, $z_1 = 0.38$ and $z_3 = 0.61$. Cosmological and non-analytically marginalised nuisance parameters, (Ω, n^nm), are fixed to their fiducial values. Left: only the Fisher part of F_2 without noise-contribution. Dashed lines after the re-parametrisation $b_{\Gamma_3} \to A_s^2 b_{\Gamma_3}$ and $c_i \to A_s c_i$ with $i \in \{0, 2, 4, \nabla^4\delta\}$. Right: only the Fisher part of F_2 with noise-terms. Dashed lines after the re-parametrisation $n_i \to A_\mathrm{AP} n_i$ with $n_i \in \{b_{\Gamma_3}, c_0, c_2, c_4, c_{\nabla^4\delta}, N, e_0, e_2\}$.

the amplitude factor due to the AP effect, which multiplies counterterms and stochastic parameters in the same way. As before, setting flat priors for those nuisance parameters introduces additional information on this AP amplitude that causes the posterior to prefer lower values of A_AP (see the right panel of figure 2) and leading to further informative priors on the parameters on which it depends: Ω_m or $\omega_\mathrm{c} - \omega_\mathrm{b} - h$ and the equation of state for dark energy $w(a)$.

In the examples above, we identified amplitudes (A_s, σ_8^2 and A_AP) which impact the terms in question (e.g., the counterterms) at all scales. In this case, eliminating projection effects in those amplitudes via re-parametrisation or via Jeffreys priors is identical: both approaches make the difference between the marginalised posterior and the profile-likelihood term in eq. (3.7) amplitude-independent. For other parameters, such as Ω_m (see figure 6 in ref. [76]), their scale-dependent impact on the power spectrum implies that determining the best amplitude to re-parametrise becomes more complex. The analogous to $\alpha = cA_\mathrm{s}$ from the paragraph above, would replace A_s with the best-measured amplitude at the scales measured by the particular experiment. We argue below for motivated combinations of σ_8 and A_AP that correspond to this for each parameter in question, but a more precise method would be to use information on uncertainties of the measurements at different scales to determine this amplitude. This information, i.e. the covariance matrix of the data, is by construction included in Jeffreys priors via the Fisher matrix. Therefore, the Jeffreys priors approach is fundamentally a more nuanced yet experiment-dependent way to eliminate projection effects, being equivalent to some more complex re-parametrisation [77]. The re-parametrisation of the amplitude-controlling parameters that we introduce here can be seen as its sub-class or a first-order approximation that is independent of the specific experiment, since the amplitudes we use are all found directly from the modelling and do not require covariance information.

JCAP04(2026)030

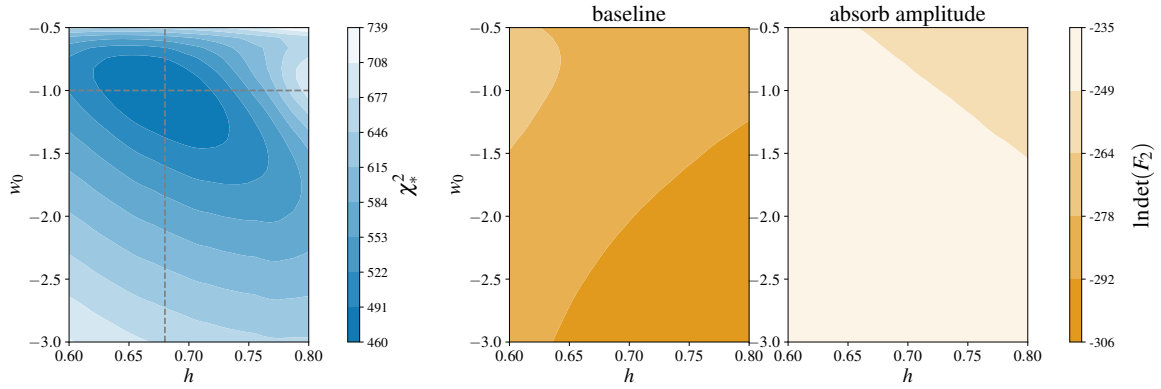

Figure 3. Impact of the re-parametrisation on the Laplace term. The computation is done with the synthetic data for the full set of BOSS multipoles. Cosmological and non-analytically marginalised nuisance parameters, $(\Omega, n^{\rm nm})$, are fixed to their fiducial values.

In beyond-ΛCDM cosmologies, extended parameters impact the evolution of structure growth and expansion history, hence affecting the amplitude signal too. For extended cosmologies which only modify the growth of structure (e.g., modified gravity models with ΛCDM background), imposing an informative prior on the primordial amplitude (e.g., from CMB measurements) might be sufficient to resolve projection effects due to the degeneracy between the extended parameters and $A_{\rm s}$ [23]. On the other hand, dark energy models modify the background expansion, opening an additional degeneracy direction and affecting the AP effect. In this scenario the arising projection effects cannot be resolved by fixing the primordial amplitude or re-parametrising nuisance parameters with $A_{\rm s}$ (or σ_8^2). While these projections do become slightly weaker with additional BAO information, they are not removed to a satisfying degree yet (see figure 3 of ref. [32]). However, when we re-define nuisance parameters to incorporate all contributions to the amplitude signal, including the AP-amplitude, we reduce the dependence of the Laplace term on the degenerate parameters (see dashed lines in figure 2), and hence the corresponding projection effects. As argued above, flat priors on the analytically marginalised parameters introduce informative priors on the cosmological parameters contributing to the AP effect. Let us demonstrate exactly that in figure 3. As we showed in the baseline analysis in figure 1, variation of the evolving dark energy parameters on noiseless ΛCDM data leads to strong biases in the expansion rate and dark energy parameters. When fixing all cosmological and non-analytically marginalised parameters to their fiducial values and varying only $w_0 - h$, the "profile likelihood" term (or the log-posterior times minus two) evaluated at the best-fit values of the analytically marginalised parameters (left panel) clearly dips around the fiducial values. Nevertheless, the minimum of the overall sum from eq. (3.7) (i.e. the maximum of the marginalised posterior) is strongly affected by the Laplace term (middle panel), which drags it to lower values of w_0 and higher values of h. This dependency is weakened when the amplitude-impacting parameters get absorbed in the nuisance parameters that appear linearly in the modelling (right panel). As per discussion above, in contrast to Jeffreys priors, this does not make the Laplace term completely independent from the cosmological parameters in question. Nevertheless, it still significantly decreases the sensitivity to them, which supports our statement of the re-parametrisation being a first-order approximation of the Jeffreys priors approach.

JCAP04(2026)030

Additionally, figure 3 can be useful to visualise the impact of projection effects on the width of the marginalised posteriors. If the contributions to the marginalised posterior distribution coming from the profile-likelihood term and from the prior-volume term have comparable significance and are in tension (i.e. they prefer different parts of the parameter space), then their combination might result not only in shifts of the parameter estimates, but also in tighter widths. In other words, the total marginalised posterior distribution has smaller volume than in the Jeffreys priors or re-parametrisation approaches. This does not mean that any information is lost when the re-parametrisation or Jeffreys priors are applied. On the contrary, broader constraints in this case would indicate that no additional information is imposed on the cosmological parameters by our choices in the nuisance parameters.

4 Re-parametrisation in full-shape analysis

4.1 BOSS DR12

After identifying and discussing the problem of projection effects in the previous section, we now investigate different amplitude controlling parameters. In this section we study how re-defining the nuisance parameters to take their impact into account mitigates the shifts in the maxima of un-marginalised and marginalised posterior distributions. The amplitude controlling parameters in question are the primordial amplitude $A_{\rm s}$, the AP amplitude $A_{\rm AP}$ (dependent on the background modifying parameters), the growth factor $D(z)$ (dependent on the structure growth modifying parameters), and σ_8 (a nonlinear function of all cosmological parameters). In table 2 we summarise different options of re-defining or re-parametrising nuisance parameters with the aforementioned amplitudes and the corresponding prior choices. In the baseline analysis, the priors on nuisance parameters are informative and motivated by the validity of the EFTofLSS approach [67, 78]. For instance, due to their perturbative nature, priors on the galaxy bias parameters beyond the linear order are following the Gaussian distribution centred at zero with standard deviation of one, i.e. $\mathcal{O}(1)$ values. We use a nonlinear scale $k_{\rm NL} = 0.45\,h/{\rm Mpc}$ and we assume an inverse number density of $\bar{n}^{-1} = 3500\,({\rm Mpc}/h)^3$ for the $z_1 = 0.38$ bin and $\bar{n}^{-1} = 5000\,({\rm Mpc}/h)^3$ for the $z_3 = 0.61$ bin. Hence, all shot noise nuisance parameters have consistent priors of the same order of magnitude to characterise deviations from the Poisson noise prediction, i.e. the inverse of the number density. Similarly to scale-dependent shot-noise, in units of the nonlinear scale, the counterterms are expected to be of $\mathcal{O}(1)$. However, the large values of velocity dispersion found in the BOSS sample [42] imply that the nonlinear scale for counterterms might be larger according to ref. [67]. This explains the choice of broad standard deviations in the quadratic and quartic countertems priors. In ref. [72] we also observed large uncertainties on counterterms with high precision numerical simulations. In general, since counterterms absorb astrophysical and other higher-order effects from smaller scales, it is difficult to derive highly informative priors from theory or numerical simulations not tailored to the actual observations. Yet it is possible to impose stricter priors from bespoke simulated galaxy catalogues based on halo occupation distribution (HOD) model [29, 30]. In this approach, the underlying galaxy-halo connection is linked to the EFTofLSS nuisance parameters, which results in physically motivated priors for different galaxy samples. However, it relies on

JCAP04(2026)030

baseline		**re-parametrisation**	
parameter	prior	parameter	prior
b_1	$[0,\ 4]$	b_1	$[0,\ 4]$
b_2	$\mathcal{N}(0,\ 1)$	b_2	$\mathcal{N}(0,\ 1)$
$b_{\mathcal{G}_2}$	$\mathcal{N}(0,\ 1)$	$b_{\mathcal{G}_2}$	$\mathcal{N}(0,\ 1)$
b_{Γ_3}	$\mathcal{N}\left(0, 1\right)$	$b_{\Gamma_3} A_{\rm AP} \times \{1, \tilde{A}_{\rm s}^2, \tilde{A}_{{\rm s},z}^2, \sigma_{8,z}^4\}$	$\mathcal{N}\left(0, \{1, 3, 2, 1\}\right)$
c_0	$\mathcal{N}(0, 30)$	$c_0 A_{\rm AP} \times \{1, \tilde{A}_{\rm s}, \tilde{A}_{{\rm s},z}, \sigma_{8,z}^2\}$	$\mathcal{N}(0, \{30, 90, 60, 30\})$
c_2	$\mathcal{N}(30, 30)$	$c_2 A_{\rm AP} \times \{1, \tilde{A}_{\rm s}, \tilde{A}_{{\rm s},z}, \sigma_{8,z}^2\}$	$\mathcal{N}(\{30, 60, 37.5, 15\}, \{30, 90, 60, 30\})$
c_4	$\mathcal{N}(0, 30)$	$c_4 A_{\rm AP} \times \{1, \tilde{A}_{\rm s}, \tilde{A}_{{\rm s},z}, \sigma_{8,z}^2\}$	$\mathcal{N}(0, \{30, 90, 60, 30\})$
$c_{\nabla^4\delta}$	$\mathcal{N}(-10^3, 10^3)$	$c_{\nabla^4\delta} A_{\rm AP} \times \{1, \tilde{A}_{\rm s}, \tilde{A}_{{\rm s},z}, \sigma_{8,z}^2\}$	$\mathcal{N}(-10^3 \cdot \{1, 2, 1.25, 0.5\}, \{1, 3, 2, 1\} \cdot 10^3)$
N	$\mathcal{N}\left(\frac{1}{\bar{n}}, \frac{2}{\bar{n}}\right)$	$N A_{\rm AP}$	$\mathcal{N}\left(\frac{1}{\bar{n}}, \frac{2}{\bar{n}}\right)$
e_0	$\mathcal{N}\left(0, \frac{2}{\bar{n} k_{\rm NL}^2}\right)$	$e_0 A_{\rm AP}$	$\mathcal{N}\left(0, \frac{2}{\bar{n} k_{\rm NL}^2}\right)$
e_2	$\mathcal{N}\left(0, \frac{2}{\bar{n} k_{\rm NL}^2}\right)$	$e_2 A_{\rm AP}$	$\mathcal{N}\left(0, \frac{2}{\bar{n} k_{\rm NL}^2}\right)$

Table 2. Setup for runs from figure 4, where $\tilde{A}_{\rm s} = A_s \times 10^9$, $\tilde{A}_{{\rm s},z} = D^2(z)/D^2_{\Lambda{\rm CDM}}(0) \times A_s \times 10^9$, $\sigma_{8,z} = D(z)/D(0)\sigma_8$. The horizontal line separates analytically marginalised parameters. Normal distributions follow linear transformation: for $X_{\rm baseline} \sim \mathcal{N}(\mu, \sigma)$, if $Y_{\rm re\text{-}parametrisation} = aX_{\rm baseline}$ then $Y_{\rm re\text{-}parametrisation} \sim \mathcal{N}(a\mu, a\sigma)$. We shift the means of the nuisance parameter priors with the rescaled fiducial values of the absorbed amplitude parameters: $A_{\rm AP,fid} = 1$, $\tilde{A}_{\rm s,fid} \approx 2.1$, $\tilde{A}_{{\rm s},z,{\rm fid}} \approx 1.25$, $\sigma^2_{8,z,{\rm fid}} \approx 0.4$. We increase the variance of the new normal distributions by a factor of 2 (for re-scaling with $\tilde{A}_{{\rm s},z}$) and 3 (for re-scaling with $\tilde{A}_{\rm s}$) to take into account values of the primordial amplitude allowed by the prior ranges in cosmological parameters.

available numerical simulations, which might insufficiently represent cosmological dependence or potentially introduce other systematic biases. For a sufficiently accurate mapping of HOD-to-EFTofLSS parameter spaces, immense number of fits must be performed, making this approach computationally expensive. Finally, matching HOD parameter space to the actual measurements is a highly non-trivial task [79–81].

In figure 4 we investigate the impact of the re-parametrisation scenarios of the analytically marginalised nuisance parameters on the noiseless BOSS DR12 synthetic data, for which the fiducial underlying cosmology is known. First, we see that absorbing the AP amplitude alone (in yellow) already brings the degenerate trio of $h - w_0 - w_a$ closer to their fiducial values. Second, addition of the primordial amplitude parameter (in green) improves the degeneracy $A_{\rm s} - h - \omega_{\rm c}$. Finally, addition of a redshift dependent components to the power spectrum amplitude, i.e. multiplication with the growth factor squared of $A_{\rm s}$ and σ_8^2 (in orange and pink, respectively) broadens the $h - w_0 - w_a$ constraints. For the rest of our analysis in this paper we choose the re-parametrisation of the analytically marginalised parameters with the time-dependent σ_8^2 and the AP amplitude (pink contours). We base this decision not on the better performance of this particular re-parametrisation in the synthetic data tests, but on the fact that it captures the amplitude signal at varying redshifts $P_\ell \propto A_{\rm AP}(z)\sigma^2(z)f(z,k)$ in a more physically motivated way than $P_\ell \propto A_{\rm AP}(z)D^2(z)A_{\rm s}f(z,k)$. Additionally, this

JCAP04(2026)030

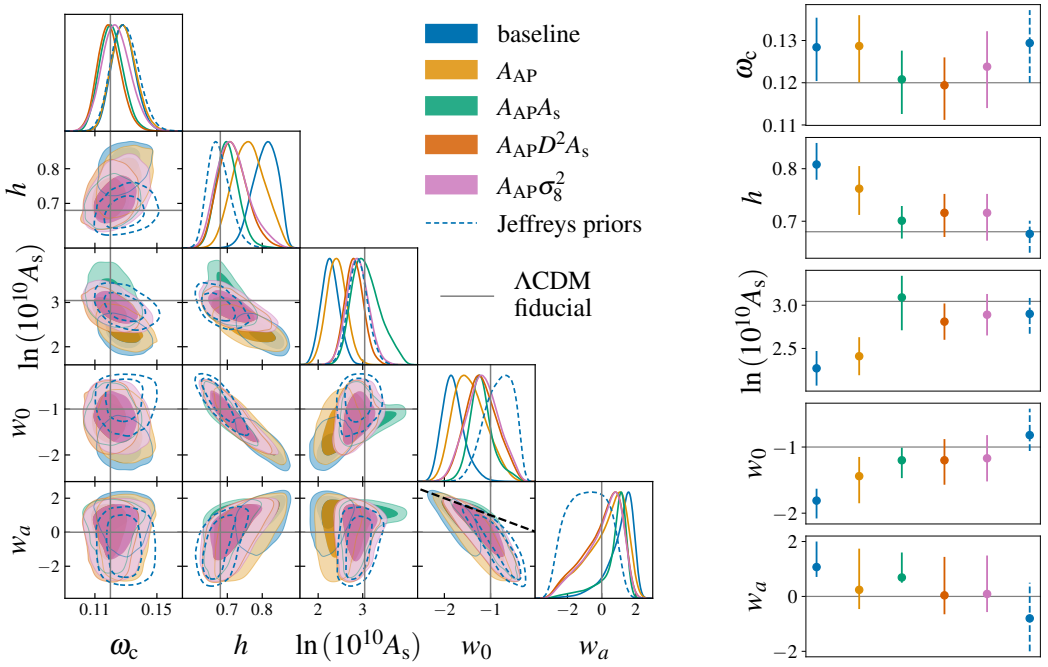

Figure 4. Different re-parametrisations of the EFTofLSS nuisance parameters and their impact on cosmological constraints demonstrated on synthetic data. *Left panel*: marginalised posterior distribution for the cosmological parameters in the w_0w_aCDM cosmology and the five re-parametrisation choices, as detailed in the legend (see table 2). Grey solid lines mark the fiducial values of the noiseless synthetic data from a fit on the BOSS DR12 multipoles in a ΛCDM scenario. *Right panel*: errorbars correspond to 68% c.l. of 1D marginalised constraints on cosmological parameters from the left panel.

re-parametrisation also proves to be more stable to the increasing prior volume due to slightly changing the degeneracy in the $A_{\rm s} - h - \omega_{\rm c}$ direction, since σ_8 is a nonlinear function of these parameters. For more details on prior-dependence see appendix B.

In figure 4 we also show the baseline analysis with the Laplace term removed via partial Jeffreys priors (dashed blue lines). Parameters h and $A_{\rm s}$, as well as w_0 and w_a recover the fiducial values correctly, without the previously observed biases in the baseline analysis (solid blue lines). There is a $\sim 1\sigma$ bias in $\omega_{\rm c}$ with respect to the fiducial value. The fact that it is not present with the re-parametrisation is possibly coincidental. As argued in section 3, with the re-parametrisation we do not make the Laplace term completely cosmology-independent, hence the residual projection effects from the analytically marginalised nuisance parameters can impact or even cancel out other intrinsic non-Gaussianities of the posterior. Overall, the fiducial cosmological parameters are always recovered within 1σ with Jeffreys priors and our chosen re-parametrisation approach. In both approaches the constraints on the evolving dark energy parameters are wider than in the baseline analysis. This demonstrates the additional consequence of projection effects discussed in the last paragraph of section 3 — constraints typically appear narrower when strong projection effects exist, but are broader when spurious information is removed.

In appendix A, we investigate versions of a "full" re-parametrisation, which includes absorbing power spectrum amplitude parameters into the galaxy bias parameters $(b_1, b_2, b_{\mathcal{G}_2})$

JCAP04(2026)030

as well. The results are very similar to the simpler re-parametrisation applied only to analytically marginalised parameters. Hence, we focus on the re-parametrisation of the parameters that appear linearly in the modelling. Another reason for this choice is to directly compare it with the Jeffreys prior approach, that in the cases shown here are only applied to linear parameters. Both approaches are easy to implement and able to mitigate prior-volume effects to a similar degree (especially for Stage IV surveys, as we argue in section 4.2). In contrast to Jeffreys priors, the re-parametrisation is independent from the particular experiment being conducted, since it is fully based on the modelling and does not depend on the covariance.

In figure 5, we show constraints on the real BOSS DR12 data, with the re-parametrisation and Jeffreys priors on the analytically marginalised parameters. The corresponding values of the posterior average and MAP are provided in table 3. Analogously to the synthetic data tests, we observe a 1σ-difference in ω_c between the approaches — both in ΛCDM and w_0w_aCDM. The constraints on the primordial amplitude agree between both approaches in both dark energy scenarios. They are also in better agreement with the Planck values of $\ln(10^{10}A_s)$ [51] than obtained in the baseline analysis (see figure 1). Constraints of the expansion rate are nearly identical in standard cosmology between both approaches. They change when the parameter space is extended to include evolving dark energy parameters. We observe a similar picture as in figure 4: h-estimate is tighter with Jeffreys priors, w_a is weakly constrained, there is a 0.8σ difference for marginalised means in w_0 between the re-parametrisation and Jeffreys priors. Overall, both approaches agree in inferred constraints on cosmological parameters and significantly reduce projection effects between the expansion rate and evolving dark energy parameters. The reduction in projection effects is also evident from the fact that cosmological parameters corresponding to the maximum of the un-marginalised posterior (values in the parenthesis, obtained with `minuit`) are close to the maxima of the marginalised posteriors in figure 4. This was not the case in previous analyses with the baseline setup (see refs. [19, 31]). Also note that when the cosmological background changes from ΛCDM to w_0w_aCDM, the central values in cosmological parameters remain unchanged within the errors, both with the re-parametrisation and Jeffreys priors. Additionally, we see very little evidence for the σ_8- or S_8-tension with respect to CMB measurements (see table 3): e.g., $S_8 = 0.832 \pm 0.013$ in ΛCDM of Planck 2018 [51]. This consistency between CMB and LSS values of S_8 holds true for standard cosmology and evolving dark energy, and agrees with the findings of DESI for DR1 FS [82] as well as with the recent results from KiDS-Legacy data [83].

4.2 Stage IV surveys

In this section we repeat the analysis on synthetic data for a DESI DR1-like setup. We re-run our analysis re-scaling the priors on the analytically marginalised parameters as $\mathcal{N}(A_{\rm fid}\mu, A_{\rm fid}\sigma)$ and show results in figure 6. For the re-scaling with the AP amplitude, we use $A_{\rm fid} = 1$, while for the re-scaling with σ_8, we have $A_{\rm fid} = \sigma^2_{8,z,{\rm fid}}$. The latter is slightly less conservative than in the same re-parametrisation for BOSS data, since it decreases the size of the priors on the analytically marginalised parameters taking the re-scaling into account. Of course, this DESI-like setup is an over-simplification of the actual DR1 setup, which includes

JCAP04(2026)030

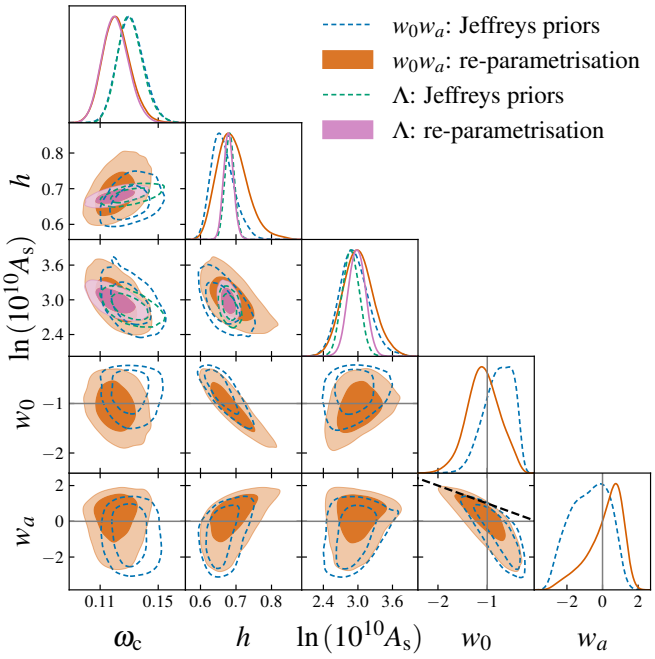

Figure 5. BOSS DR12 FS constraints with the re-parametrisation and Jeffreys priors of the analytically marginalised parameters in the standard cosmology and evolving dark energy. Grey solid lines denote the ΛCDM limit with $w_0 = -1$ and $w_a = 0$.

	re-parametrisation		**Jeffreys priors**	
	ΛCDM	w_0w_aCDM	ΛCDM	w_0w_aCDM
ω_c	$0.121^{+0.008}_{-0.009}$ (0.124)	$0.121^{+0.008}_{-0.010}$ (0.122)	$0.131^{+0.008}_{-0.009}$ (0.128)	$0.131^{+0.008}_{-0.009}$ (0.126)
h	$0.679^{+0.013}_{-0.014}$ (0.676)	$0.690^{+0.034}_{-0.048}$ (0.673)	0.682 ± 0.014 (0.681)	$0.663^{+0.025}_{-0.037}$ (0.649)
$\ln(10^{10}A_s)$	2.98 ± 0.15 (2.92)	$3.00^{+0.25}_{-0.28}$ (3.25)	2.88 ± 0.15 (2.93)	$2.94^{+0.22}_{-0.27}$ (3.16)
w_0	-1	-1.08 ± 0.33 (-1.12)	-1	$-0.77^{+0.43}_{-0.16}$ (-0.81)
w_a	0	$0.16^{+1.20}_{-0.55}$ (0.96)	0	$-0.72^{+1.30}_{-0.99}$ (0.03)
σ_8	0.783 ± 0.050 (0.770)	0.784 ± 0.053 (0.797)	$0.785^{+0.048}_{-0.054}$ (0.798)	$0.788^{+0.055}_{-0.064}$ (0.829)
S_8	0.798 ± 0.054 (0.798)	$0.791^{+0.068}_{-0.077}$ (0.824)	0.825 ± 0.056 (0.832)	0.854 ± 0.081 (0.900)

Table 3. Mean values and 68% c.l. values for ΛCDM and evolving dark energy with fixed neutrino mass $M_\nu = 0.06\,\text{eV}$ for the FS analysis of BOSS data, using the re-parametrisation and Jeffreys priors on analytically marginalised parameters. We do not show constraints on n_s and ω_b as they are completely prior-dominated. We add the maximum values of the un-marginalised posterior in parentheses, and include derived constraints on σ_8 and S_8.

JCAP04(2026)030

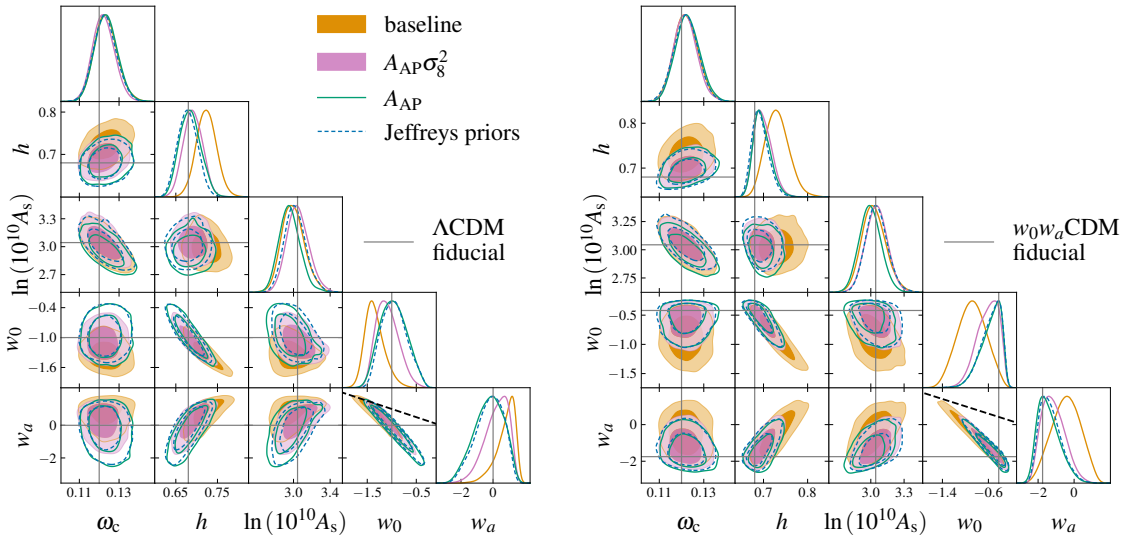

Figure 6. Constraining evolving dark energy with synthetic DESI DR1-like data using different FS analysis choices, as specified in the legend (see table 5 and the main text for details on the nuisance parameter priors). *Left panel*: marginalised posterior distribution for cosmological parameters with the fiducial ΛCDM cosmology. *Right panel*: similar to the left panel but with the fiducial w_0w_aCDM cosmology. Grey solid lines mark the fiducial values of the noiseless synthetic data.

more redshift bins and a non-Gaussian covariance. However, this proof of concept resembles the official DESI findings [32] in the baseline analysis. It also shows how robustly our simple re-parametrisation works and effectively re-creates the impact of Jeffreys priors. Additionally, it demonstrates that for measurements with projections less severe than in BOSS for $\omega_c - A_s$, re-scaling with the AP-amplitude might suffice to mitigate $w_0 - w_a - h$ projection effects. Finally, to avoid any bias towards the standard cosmology due to the synthetic data-vectors setup, we demonstrate that our re-parametrisation approach works well for a fiducial evolving dark energy scenario too. In this case we set fiducial values for the dark energy parameters to $w_0 = -0.42$ and $w_a = -1.75$, the central values for the deviation from the standard cosmology found in the DESI DR2 BAO+CMB analysis [64]. In the right panel of figure 6, we again observe an effective mitigation of the projection effects with the re-parametrisation.

5 BOSS DR12 full-shape and other probes

5.1 BAO

After developing and assessing the re-parametrisation approach in the FS analysis, we proceed with constraining evolving dark energy exclusively with pre-DESI LSS probes. First, we contemplate the question whether a FS analysis adds any information on background parameters compared to BAO alone. For this we take four α's from the same sky-cuts as our multipoles and fit background parameters keeping the BBN prior on the baryonic density. It is evident from figure 7 that constraints on $w_0 - w_a$ are not purely driven by the information in BAO for BOSS, but FS adds constraining power. The FS analysis provides an additional channel to extract information on $\Omega_{\rm m}$, which is relevant for the degeneracies between the

JCAP04(2026)030

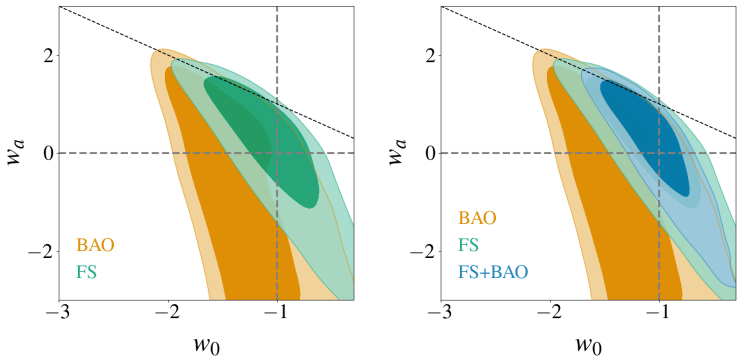

Figure 7. Constraining the evolving dark energy parameters with BOSS DR12 probes: BAO and FS alone (left panel) and together with their combination (right panel). Grey dashed lines mark the ΛCDM limit, black dashed lines denote the condition $w_0 + w_a < 0$.

evolving dark energy and background evolution parameters. With mitigated projection effects, not only does FS slightly change the degeneracy direction in $w_0 - w_a$, but also improves constraints on the time-evolving component w_a. This is significant for the BOSS setup, as it contains only two redshift bins $z_1 = 0.38$ and $z_3 = 0.61$: i.e. two degrees of freedom in $w(z)$ per two redshifts. It might be interesting to asses the contribution of FS to the BAO constraints of the evolving dark energy parameters in the DESI setup. There, BAO- and FS-measurements span a much broader range of redshifts and the precision of measurements is also significantly improved with respect to BOSS.

5.2 External large-scale structure probes: BAO and DES Y3

After highlighting the value of adding FS information to a BAO-only analysis, we also combine with additional external probes. The resulting constraints on evolving dark energy are shown in figure 8, while numerical values are provided in table 4. The addition of external BAO measurements from lower and higher redshifts than BOSS starts shifting the contours to the parameter space preferred by DESI (central panel of figure 8). This happens only if the higher redshift BAO measurements are included in the analysis, providing an anchor in the time evolution. For discussions on the evolving dark energy signatures in DESI see, e.g., refs. [84–89].

Lastly, we combine Stage III spectroscopic probes with photometric measurements from DES Y3 (left panel of figure 8). Note a similar behaviour in the right panel of figure 14 in DESI DR2 BAO analysis [64]: there the authors replace the CMB with the DES Y3 information, to obtain a constraint coming entirely from low-redshift LSS probes. They also observe that this combination favours the same region of parameter space. For comparison we include contours for a repeated DESI analysis, which in the official collaboration paper constrains evolving dark energy parameters to $w_0 = -0.752 \pm 0.057$, $w_a = -0.86^{+0.23}_{-0.20}$ (DESI DR2 BAO+CMB+DESY5) [64]. DESI DR1 FS analysis required inclusion of SN, obtaining similar constraints: $w_0 = -0.761 \pm 0.065$, $w_a = -1.02^{+0.3}_{-0.26}$ (DESI DR1 FS+BAO+CMB+DESY5) [82]. These values remain nearly unchanged if one substitutes DESI DR1 FS with BOSS/eBOSS BAO measurements: $w_0 = -0.761 \pm 0.064$,

JCAP04(2026)030

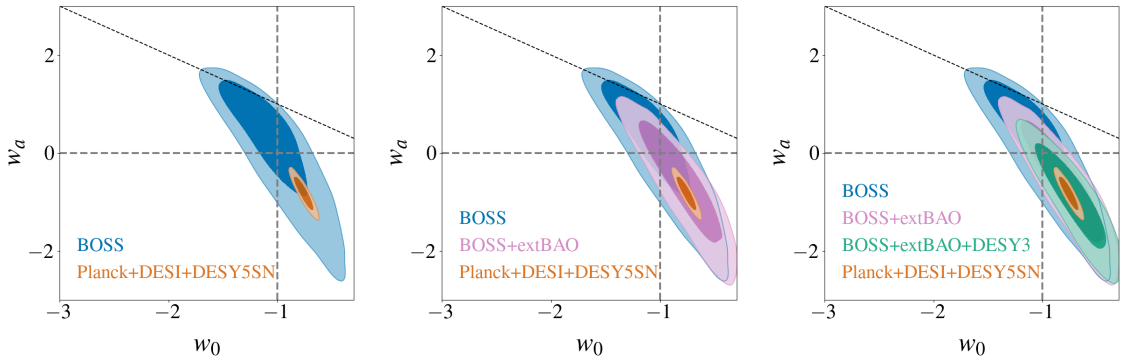

Figure 8. Constraining the evolving dark energy parameters with BOSS and external probes: BOSS DR12 FS+BAO (left panel in blue), BOSS and external BAO measurements (middle panel in pink), BOSS and external BAO with the photometric probes from DES Y3 (right panel in green). For comparison, the orange contours presents constraints from DESI DR2 BAO with the CMB and SN from DES Y5. Grey dashed lines mark the ΛCDM limit, black dashed lines denote the condition $w_0+w_a < 0$.

	BOSS BAO	BOSS FS+BAO	BOSS+extBAO	BOSS+extBAO+DES
ω_c	$0.249^{+0.073}_{-0.053}$ (0.280)	$0.121^{+0.008}_{-0.010}$ (0.122)	$0.116^{+0.007}_{-0.009}$ (0.117)	$0.119^{+0.005}_{-0.006}$ (0.120)
h	$0.800^{+0.071}_{-0.026}$ (0.87)	$0.688^{+0.030}_{-0.035}$ (0.673)	$0.660^{+0.021}_{-0.028}$ (0.648)	$0.659^{+0.019}_{-0.023}$ (0.647)
$\ln(10^{10}A_s)$	-	$3.03^{+0.20}_{-0.24}$ (3.05)	3.05 ± 0.18 (3.02)	2.99 ± 0.10 (2.99)
w_0	$-1.34^{+0.33}_{-0.47}$ (−1.9)	$-1.06^{+0.23}_{-0.31}$ (−1.02)	-0.80 ± 0.24 (−0.68)	-0.72 ± 0.21 (−0.64)
w_a	< 0.169 (−0.8)	$0.22^{+1.10}_{-0.46}$ (0.44)	$-0.63^{+0.92}_{-0.72}$ (−0.90)	$-0.91^{+0.78}_{-0.64}$ (−1.03)
σ_8	-	0.786 ± 0.049 (0.783)	0.777 ± 0.048 (0.768)	0.773 ± 0.023 (0.765)
S_8	-	0.793 ± 0.058 (0.809)	0.801 ± 0.055 (0.810)	0.809 ± 0.016 (0.818)

Table 4. Mean values and 68% c.l. values for the w_0w_aCDM cosmology with fixed neutrino mass $M_\nu = 0.06\,\mathrm{eV}$ for BOSS BAO (with the upper bound on w_a referring to the 68% limit), FS+BAO with BOSS, their combination with external BAO measurements, as well as with DES Y3 $3\times2\,\mathrm{pt}$ analysis. We show the best-fit values in parentheses, and include derived constraints on σ_8 and S_8.

$w_a = -0.88^{+0.29}_{-0.25}$ (DESI DR1 BAO + SDSS BAO + CMB + DESY5) [90]. Our purely Stage III LSS driven constraints,

$$\left.\begin{aligned} w_0 &= -0.72 \pm 0.21 \\ w_a &= -0.91^{+0.78}_{-0.64} \end{aligned}\right\} \quad \text{BOSS+extBAO+DESY3}, \tag{5.1}$$

are in good agreement with DESI results, hinting at a potential deviation from standard cosmology but with larger uncertainties and less significance.

Moreover, similar to our previous work [31], we advocate for the joint analysis of spectroscopic and photometric probes: FS+BAO+3×2 pt. This combination provides a level of constraining power comparable to the addition of CMB information to the spectroscopic analysis. For instance, in ref. [91] the authors find constraints similar to ours of $w_0 = -0.72^{+0.09}_{-0.11}$ and $w_a = -0.91^{+0.42}_{-0.33}$ for smooth quintessence, i.e. evolving dark energy without clustering. They use a similar set of probes: BOSS DR12 EFTofLSS baseline FS and bispectrum (which presumably mitigates projections) at one-loop level, with external BAO (nearly the same as

JCAP04(2026)030

ours, the high redshift ones are eBOSS DR14 instead of DR16), and Planck instead of DES Y3. Last but not least, a comparison to the official BOSS DR12 results: with the inclusion of CMB information from Planck, FS+BAO (with no extBAO) constrain $w_0 = -0.68 \pm 0.18$ and $w_a = -0.98 \pm 0.53$ [92]. Note that FS in this case is not the EFTofLSS approach of fitting the multipoles, but a compression of the multipoles and clustering wedges statistics, in configuration and Fourier space, into the following properties [93–96]: $D_{\rm M}(z)/r_{\rm d}$, $H(z)r_{\rm d}$, $f(z)\sigma_8(z)$. These different approaches are later combined in a consensus set and then used in the analysis. Additionally, in this analysis no projection effects were observed, as the different methodologies applied to BOSS data resulted in posteriors that were well described by Gaussian multivariate distributions. The redshift binning is also different: it includes an additional intermediate z-bin, $z_2 = 0.51$. Agreement with these Stage III constraints, while not manifesting a significant deviation from ΛCDM, showcases a successful application of our re-parametrisation in FS analysis.

6 Conclusion

The goal of this paper is two-fold: (1) to present a simple re-parametrisation approach for the EFTofLSS full-shape analysis to mitigate projection effects, and (2) to apply this method in combination with other external probes from Stage III large-scale low-redshift measurements (pre-DESI). First, we pedagogically introduced projection or prior-volume effects. These effects manifest themselves through shifts in the marginalised posterior maxima from the corresponding best-fit values of the un-marginalised posterior. In general, they affect any non-Gaussian multi-dimensional posterior distribution that is compressed into a lower dimensional parameter space. In case of the full-shape approach this comes from the degeneracy between cosmological, extended (beyond-ΛCDM) and the EFTofLSS nuisance parameters — all of them affecting the amplitude of the measured power spectrum multipoles. We introduce a re-parameterisation of the EFTofLSS nuisance parameters with the amplitudes $A_{\rm AP}\sigma^2_{8,z}$ (the Alcock-Paczynski amplitude times the variance of the density field, smoothed within $8\,{\rm Mpc}\,h^{-1}$ and re-scaled with the time-dependent growth factor), and show it weakens the impact of projection effects. We tested this approach on synthetic noiseless data generated for BOSS DR12 and DESI DR1 setups in the evolving dark energy scenario, w_0w_aCDM. For both setups, we compared the performance of the re-parametrisation to an alternative method of mitigating projection effects — Jeffreys priors. Imposing such priors and re-parametrising the same set of the nuisance parameters, both approaches showed a good level of agreement. The advantages of the re-parametrisation approach: it is simple to implement and interpret, straightforward to extend to nuisance parameters which appear nonlinearly in the model, and is independent from the particular experiment because it is fully based on the modelling and does not depend on the covariance. It also allows the use of priors on nuisance parameters motivated by the validity of the EFTofLSS with caution to our limited understanding of astrophysical and nonlinear effects. Beyond the purely frequentist approach (for instance, see the recent ref. [97]), the re-parametrisation is one of the simplest ways to measure evolving dark energy with mitigated prior-volume effects in the Bayesian framework.

In the second half of the paper, we focused on constraining evolving dark energy with Stage III publicly available data: BOSS DR12 (power spectrum multipoles and BAO), external

JCAP04(2026)030

BAO measurements (from 6DF, SDSS DR7 MGC and eBOSS DR16 surveys), and the $3\times2\,\mathrm{pt}$ correlation functions of DES Y3. We found that, for BOSS data, the full-shape analysis with the re-parametrisation adds information on dark energy parameters with respect to the BAO-only analysis. We also found that adding BAO information from redshifts higher than those covered by BOSS drives the constraints into the parameter region preferred by DESI, namely $w_0 > -1$ and $w_a < 0$. Finally, when combining all probes together under the application of the re-parametrisation in the full-shape analysis, we obtained the following constraints of the evolving dark energy parameters: $w_0 = -0.72 \pm 0.21$ and $w_a = -0.91^{+0.78}_{-0.64}$. To our knowledge, these are the first purely large-scale structure pre-DESI constraints in the w_0w_aCDM cosmology. They are also in good agreement with the official BOSS DR12 results [92] and a recent analysis with the one-loop bispectrum [91] — both analyses include CMB information from Planck instead of the $3\times2\,\mathrm{pt}$ correlation functions of DES Y3. Although our constraints do not indicate a significant deviation from ΛCDM, they still demonstrate robustness of our re-parametrisation and potential of exclusively late-time Universe constraints.

The methods and findings of this study are important for forthcoming beyond-ΛCDM analyses by Stage IV surveys like DESI, Euclid, Rubin, and their combinations.

A Full re-parametrisation

In a full re-parametrisation of the EFTofLSS nuisance parameters, not analytically marginalised galaxy bias parameters also re-absorb an amplitude parameter. Similar to DESI's approach, we obtain $b_1 \to b_1\sigma_{8,z}$ and $b_{2,\mathcal{G}_2} \to b_{2,\mathcal{G}_2}\sigma^2_{8,z}$. To take the AP-amplitude into account (e.g., in term like $b_1^2 A_{\rm AP} P_{\rm L}$) we add a square-root of it to the newly defined galaxy bias parameters. Note that we have various powers of these galaxy bias parameters in the model. Hence, the cancellation of the amplitude-controlling parameters will not be as straightforward as in the case of the analytically marginalised parameters, which appear only linearly in the EFTofLSS. We also note that in the analytically marginalised part we have certain terms multiplied with the Kaiser term, i.e. $b_{\Gamma_3}(b_1+f\mu^2)P_{13}$ and $c_{\nabla^4\delta}(b_1+f\mu^2)^2P_{\rm L}$. Therefore, we distinguish between two full re-parametrisation approaches: (a) one where the Kaiser term is taken into account, i.e. only the leading order terms, $b_{\Gamma_3}b_1A_{\rm AP}P_{\rm L}^2$ and $c_{\nabla^4\delta}b_1^2A_{\rm AP}P_{\rm L}$, are multiplied with the amplitude; (b) one where we use the same re-parametrisation of the analytically marginalised parameters as before in table 2. All options are summarised in table 5. The results from synthetic BOSS data are shown in figure 9. The priors applied in the analyses for each option in figure 9 are identical to the $A_{\rm AP}\sigma^2_{8,z}$ re-parametrisation analysis from table 2. We see that all approaches are consistent between each other. The best agreement with the fiducial cosmology is reached by the full re-parametrisation in which the AP-amplitude is absorbed in all nuisance parameters and the analytically marginalised parameters are treated in the same way as presented in table 2. Additionally, in the next section we demonstrate stability of this re-parametrisation to changes of the prior-volume.

B Prior-dependence

In appendix of ref. [19], the authors demonstrate a strong dependence of cosmological constraints on the size of the EFTofLSS priors. We repeatedly vary the size of the Gaussian

JCAP04(2026)030

"Kaiser term" re-parametrisation		**"ignore Kaiser term" re-parametrisation**	
full+Kaiser	full+Kaiser+AP	full	full+AP
$b_1\sigma_{8,z}$	$b_1\sigma_{8,z}\sqrt{A_{\rm AP}}$	$b_1\sigma_{8,z}$	$b_1\sigma_{8,z}\sqrt{A_{\rm AP}}$
$b_2\sigma^2_{8,z}$	$b_2\sigma^2_{8,z}\sqrt{A_{\rm AP}}$	$b_2\sigma^2_{8,z}$	$b_2\sigma^2_{8,z}\sqrt{A_{\rm AP}}$
$b_{\mathcal{G}_2}\sigma^2_{8,z}$	$b_{\mathcal{G}_2}\sigma^2_{8,z}\sqrt{A_{\rm AP}}$	$b_{\mathcal{G}_2}\sigma^2_{8,z}$	$b_{\mathcal{G}_2}\sigma^2_{8,z}\sqrt{A_{\rm AP}}$
$b_{\Gamma_3}A_{\rm AP}\sigma^3_{8,z}$	$b_{\Gamma_3}\sqrt{A_{\rm AP}}\sigma^3_{8,z}$	$b_{\Gamma_3}A_{\rm AP}\sigma^4_{8,z}$	$b_{\Gamma_3}A_{\rm AP}\sigma^4_{8,z}$
$c_0A_{\rm AP}\sigma^2_{8,z}$	$c_0A_{\rm AP}\sigma^2_{8,z}$	$c_0A_{\rm AP}\sigma^2_{8,z}$	$c_0A_{\rm AP}\sigma^2_{8,z}$
$c_2A_{\rm AP}\sigma^2_{8,z}$	$c_2A_{\rm AP}\sigma^2_{8,z}$	$c_2A_{\rm AP}\sigma^2_{8,z}$	$c_2A_{\rm AP}\sigma^2_{8,z}$
$c_4A_{\rm AP}\sigma^2_{8,z}$	$c_4A_{\rm AP}\sigma^2_{8,z}$	$c_4A_{\rm AP}\sigma^2_{8,z}$	$c_4A_{\rm AP}\sigma^2_{8,z}$
$c_{\nabla^4\delta}A_{\rm AP}$	$c_{\nabla^4\delta}$	$c_{\nabla^4\delta}A_{\rm AP}\sigma^2_{8,z}$	$c_{\nabla^4\delta}A_{\rm AP}\sigma^2_{8,z}$
$NA_{\rm AP}$	$NA_{\rm AP}$	$NA_{\rm AP}$	$NA_{\rm AP}$
$e_0A_{\rm AP}$	$e_0A_{\rm AP}$	$e_0A_{\rm AP}$	$e_0A_{\rm AP}$
$e_2A_{\rm AP}$	$e_2A_{\rm AP}$	$e_2A_{\rm AP}$	$e_2A_{\rm AP}$

Table 5. Various options to re-parametrise the EFTofLSS nuisance parameters, both analytically marginalised and sampled explicately (separated by the horizontal line).

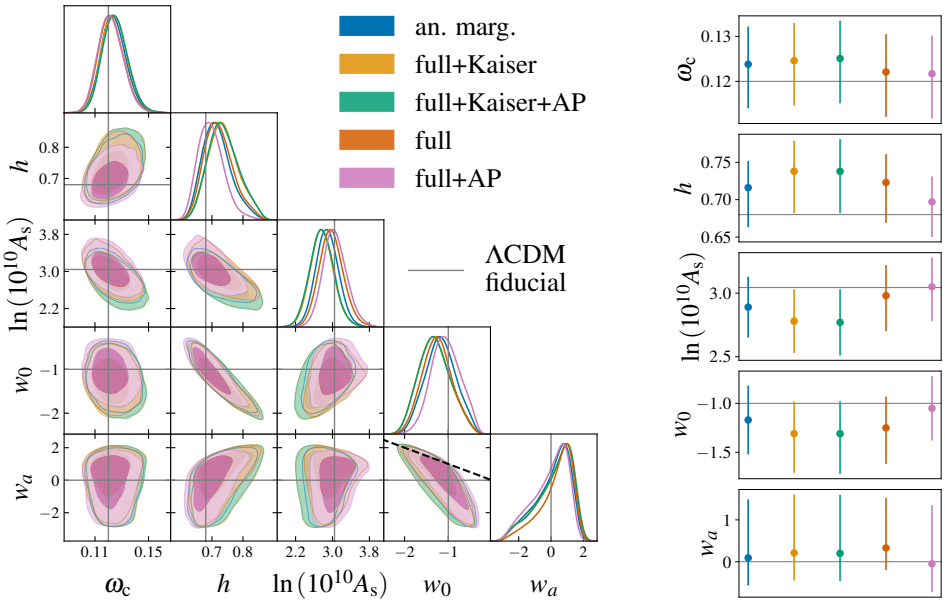

Figure 9. Different re-parametrisations of the EFTofLSS nuisance parameters and their impact on cosmological constraints demonstrated on synthetic data. *Left panel*: marginalised posterior distribution for the cosmological parameters in the w_0w_aCDM cosmology and the five re-parametrisation choices, as detailed in the legend (blue colour denotes the case of $A_{\rm AP}\sigma^2_{8,z}$ re-scaling of the analytically marginalised parameters from table 2, other colours denote the options from table 5). Grey solid lines mark the fiducial values of the noiseless synthetic data from a fit on the BOSS DR12 multipoles in a ΛCDM scenario. *Right panel*: errorbars correspond to 68% c.l. of 1D marginalised constraints on cosmological parameters from the left panel.

JCAP04(2026)030

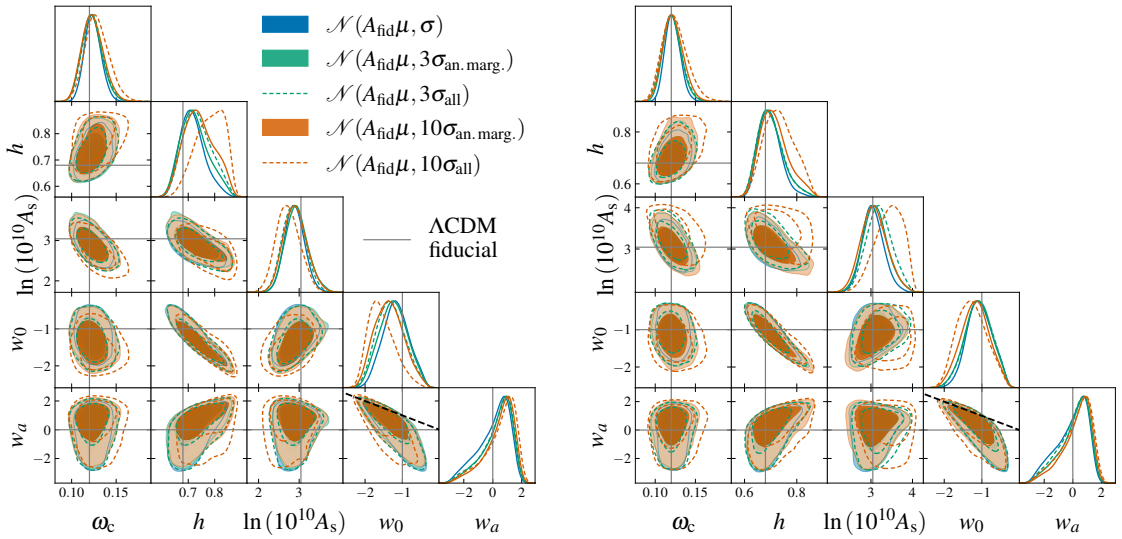

Figure 10. Different size of priors of the EFTofLSS nuisance parameters and their impact on cosmological constraints demonstrated on synthetic data. *Left panel*: re-parametrisation of the analytically marginalised parameters. *Right panel*: full re-parametrisation ("full+AP" in figure 9), same colour scheme as in the left panel. *Legend*: the short-hand notation for varying size of the Gaussian priors includes $\mathcal{N}$ with the average μ and σ from the baseline analysis, $A_{\rm fid}$ is the re-scaling factor of the prior-means in the re-parametrisation with $A_{\rm AP}\sigma^2_{8,z}$ (see table 2), $\sigma_{\rm an.\,marg.}$ denotes increased priors only in the analytically marginalised parameters, while $\sigma_{\rm all}$ denotes increased priors in all nuisance parameters.

priors on the nuisance parameters in our re-parametrisation on the ΛCDM synthetic BOSS-data here. The only difference with respect to ref. [19], is imposing a $10\sigma_{\rm Planck}$ prior on $n_{\rm s}$. In figure 10 we demonstrate that the re-parametrisation with $A_{\rm AP}\sigma^2_{8,z}$ is nearly prior-independent. One can see only slight shifts when priors on the analytically marginalised parameters are increased. The only case of notable shifts is when priors on $b_{\mathcal{G}_2}$ and b_2 are increased 10 times: in $w_0 - h$ for the re-parametrisation of the analytically marginalised parameters and in $h - \ln(10^{10}A_{\rm s})$ for the full re-parametrisation. Both these scenarios correspond to fairly unrealistic values for perturbative galaxy biases.

Acknowledgments

We thank Alkistis Pourtsidou for useful discussions and an MCMC chain with the DESI DR2 BAO re-analysis. We thank Joe Zuntz for valuable comments. We also thank Samuel Brieden for recommendations on the DESI DR1-like setup and Marco Bonici for a discussion on HOD-informed priors. The authors are grateful to the BOSS and DES collaborations for making their data publicly available. We acknowledge use of the Cuillin computing cluster of the Royal Observatory, University of Edinburgh. MT's research is supported by grant ST/Y000986/1. PC's research was supported by grant RF/ERE/221061 in the initial stages of this work. For the purpose of open access, the author has applied a Creative Commons Attribution (CC BY) licence to any Author Accepted Manuscript version arising from this submission.

JCAP04(2026)030

References

[1] BOSS collaboration, *The Baryon Oscillation Spectroscopic Survey of SDSS-III*, *Astron. J.* **145** (2013) 10 [arXiv:1208.0022] [INSPIRE].

[2] S. Alam et al., *Completed SDSS-IV extended Baryon Oscillation Spectroscopic Survey: Cosmological implications from two decades of spectroscopic surveys at the Apache Point Observatory*, *Phys. Rev. D* **103** (2021) 083533 [arXiv:2007.08991] [INSPIRE].

[3] DESI collaboration, *The DESI Experiment Part I: Science, Targeting, and Survey Design*, arXiv:1611.00036 [INSPIRE].

[4] P.J.E. Peebles, *The large-scale structure of the universe*, Princeton University Press (1980).

[5] D.J. Eisenstein, W. Hu and M. Tegmark, *Cosmic complementarity: H_0 and Ω_m from combining CMB experiments and redshift surveys*, *Astrophys. J. Lett.* **504** (1998) L57 [astro-ph/9805239] [INSPIRE].

[6] S. Alam et al., *Towards testing the theory of gravity with DESI: summary statistics, model predictions and future simulation requirements*, *JCAP* **11** (2021) 050 [arXiv:2011.05771] [INSPIRE].

[7] D. Huterer, *Growth of cosmic structure*, *Astron. Astrophys. Rev.* **31** (2023) 2 [arXiv:2212.05003] [INSPIRE].

[8] D. Baumann, A. Nicolis, L. Senatore and M. Zaldarriaga, *Cosmological Non-Linearities as an Effective Fluid*, *JCAP* **07** (2012) 051 [arXiv:1004.2488] [INSPIRE].

[9] J.J.M. Carrasco, M.P. Hertzberg and L. Senatore, *The Effective Field Theory of Cosmological Large Scale Structures*, *JHEP* **09** (2012) 082 [arXiv:1206.2926] [INSPIRE].

[10] A. Perko, L. Senatore, E. Jennings and R.H. Wechsler, *Biased Tracers in Redshift Space in the EFT of Large-Scale Structure*, arXiv:1610.09321 [INSPIRE].

[11] L. Fonseca de la Bella, D. Regan, D. Seery and S. Hotchkiss, *The matter power spectrum in redshift space using effective field theory*, *JCAP* **11** (2017) 039 [arXiv:1704.05309] [INSPIRE].

[12] G. D'Amico et al., *The Cosmological Analysis of the SDSS/BOSS data from the Effective Field Theory of Large-Scale Structure*, *JCAP* **05** (2020) 005 [arXiv:1909.05271] [INSPIRE].

[13] R.C. Nunes et al., *New tests of dark sector interactions from the full-shape galaxy power spectrum*, *Phys. Rev. D* **105** (2022) 123506 [arXiv:2203.08093] [INSPIRE].

[14] L. Piga et al., *Constraints on modified gravity from the BOSS galaxy survey*, *JCAP* **04** (2023) 038 [arXiv:2211.12523] [INSPIRE].

[15] P. Taule et al., *Constraints on dark energy and modified gravity from the BOSS Full-Shape and DESI BAO data*, *JCAP* **03** (2025) 036 [arXiv:2409.08971] [INSPIRE].

[16] G. D'Amico, L. Senatore and P. Zhang, *Limits on wCDM from the EFTofLSS with the PyBird code*, *JCAP* **01** (2021) 006 [arXiv:2003.07956] [INSPIRE].

[17] R. Gsponer et al., *Cosmological constraints on early dark energy from the full shape analysis of eBOSS DR16*, *Mon. Not. Roy. Astron. Soc.* **530** (2024) 3075 [arXiv:2312.01977] [INSPIRE].

[18] M.M. Ivanov et al., *Full-shape analysis with simulation-based priors: Constraints on single field inflation from BOSS*, *Phys. Rev. D* **110** (2024) 063538 [arXiv:2402.13310] [INSPIRE].

[19] P. Carrilho, C. Moretti and A. Pourtsidou, *Cosmology with the EFTofLSS and BOSS: dark energy constraints and a note on priors*, *JCAP* **01** (2023) 028 [arXiv:2207.14784] [INSPIRE].

JCAP04(2026)030

[20] T. Simon, P. Zhang, V. Poulin and T.L. Smith, *Consistency of effective field theory analyses of the BOSS power spectrum*, *Phys. Rev. D* **107** (2023) 123530 [arXiv:2208.05929] [INSPIRE].

[21] A. Gómez-Valent, *Fast test to assess the impact of marginalization in Monte Carlo analyses and its application to cosmology*, *Phys. Rev. D* **106** (2022) 063506 [arXiv:2203.16285] [INSPIRE].

[22] B. Hadzhiyska et al., *Cosmology with 6 parameters in the Stage-IV era: efficient marginalisation over nuisance parameters*, *Open J. Astrophys.* **6** (2023) 23 [arXiv:2301.11895] [INSPIRE].

[23] C. Moretti, M. Tsedrik, P. Carrilho and A. Pourtsidou, *Modified gravity and massive neutrinos: constraints from the full shape analysis of BOSS galaxies and forecasts for Stage IV surveys*, *JCAP* **12** (2023) 025 [arXiv:2306.09275] [INSPIRE].

[24] M. Maus et al., *An analysis of parameter compression and Full-Modeling techniques with Velocileptors for DESI 2024 and beyond*, *JCAP* **01** (2025) 138 [arXiv:2404.07312] [INSPIRE].

[25] H. Jeffreys, *An invariant form for the prior probability in estimation problems*, *Proc. Roy. Soc. Lond. A* **186** (1946) 453.

[26] J. Donald-McCann et al., *Analysis of unified galaxy power spectrum multipole measurements*, *Mon. Not. Roy. Astron. Soc.* **526** (2023) 3461 [arXiv:2307.07475] [INSPIRE].

[27] R. Zhao et al., *A multitracer analysis for the eBOSS galaxy sample based on the effective field theory of large-scale structure*, *Mon. Not. Roy. Astron. Soc.* **532** (2024) 783 [arXiv:2308.06206] [INSPIRE].

[28] S. Paradiso et al., *Reducing nuisance prior sensitivity via non-linear reparameterization, with application to EFT analyses of large-scale structure*, *JCAP* **07 (2025) 005** [arXiv:2412.03503] [INSPIRE].

[29] H. Zhang et al., *HOD-informed prior for EFT-based full-shape analyses of LSS*, *JCAP* **04** (2025) 041 [arXiv:2409.12937] [INSPIRE].

[30] DESI collaboration, *Enhancing DESI DR1 full-shape analyses using HOD-informed priors*, *JCAP* **11** (2025) 049 [arXiv:2504.10407] [INSPIRE].

[31] M. Tsedrik et al., *Interacting dark energy constraints from the full-shape analyses of BOSS DR12 and DES Year 3 measurements*, *Mon. Not. Roy. Astron. Soc.* **541** (2025) L65 [arXiv:2502.03390] [INSPIRE].

[32] DESI collaboration, *DESI 2024 V: Full-Shape galaxy clustering from galaxies and quasars*, *JCAP* **09** (2025) 008 [*Erratum ibid.* **02** (2026) E02] [arXiv:2411.12021] [INSPIRE].

[33] A. Chudaykin, M.M. Ivanov and O.H.E. Philcox, *Reanalyzing DESI DR1. I. ΛCDM constraints from the power spectrum and bispectrum*, *Phys. Rev. D* **113** (2026) 063502 [arXiv:2507.13433] [INSPIRE].

[34] A. Chudaykin, M.M. Ivanov and O.H.E. Philcox, *Reanalyzing DESI DR1: 2. Constraints on Dark Energy, Spatial Curvature, and Neutrino Masses*, arXiv:2511.20757 [INSPIRE].

[35] DES collaboration, *Dark Energy Survey year 3 results: Constraints on cosmological parameters and galaxy-bias models from galaxy clustering and galaxy-galaxy lensing using the redMaGiC sample*, *Phys. Rev. D* **106** (2022) 043520 [arXiv:2105.13545] [INSPIRE].

[36] DES collaboration, *Dark Energy Survey Year 3 results: Cosmological constraints from galaxy clustering and galaxy-galaxy lensing using the MagLim lens sample*, *Phys. Rev. D* **106** (2022) 103530 [arXiv:2105.13546] [INSPIRE].

[37] C. Alcock and B. Paczynski, *An evolution free test for non-zero cosmological constant*, *Nature* **281** (1979) 358 [INSPIRE].

JCAP04(2026)030

[38] J.U. Lange, *nautilus: boosting Bayesian importance nested sampling with deep learning*, *Mon. Not. Roy. Astron. Soc.* **525** (2023) 3181 [arXiv:2306.16923] [INSPIRE].

[39] A. Lewis, *GetDist: a Python package for analysing Monte Carlo samples*, *JCAP* **08** (2025) 025 [arXiv:1910.13970] [INSPIRE].

[40] S. Alam et al., *The Eleventh and Twelfth Data Releases of the Sloan Digital Sky Survey: Final Data from SDSS-III*, *Astrophys. J. Suppl.* **219** (2015) 12 [arXiv:1501.00963] [INSPIRE].

[41] H. Gil-Marín et al., *The clustering of galaxies in the SDSS-III Baryon Oscillation Spectroscopic Survey: RSD measurement from the LOS-dependent power spectrum of DR12 BOSS galaxies*, *Mon. Not. Roy. Astron. Soc.* **460** (2016) 4188 [arXiv:1509.06386] [INSPIRE].

[42] F. Beutler et al., *The clustering of galaxies in the completed SDSS-III Baryon Oscillation Spectroscopic Survey: Anisotropic galaxy clustering in Fourier-space*, *Mon. Not. Roy. Astron. Soc.* **466** (2017) 2242 [arXiv:1607.03150] [INSPIRE].

[43] O.H.E. Philcox and M.M. Ivanov, *BOSS DR12 full-shape cosmology: ΛCDM constraints from the large-scale galaxy power spectrum and bispectrum monopole*, *Phys. Rev. D* **105** (2022) 043517 [arXiv:2112.04515] [INSPIRE].

[44] O.H.E. Philcox, *Cosmology without window functions: Quadratic estimators for the galaxy power spectrum*, *Phys. Rev. D* **103** (2021) 103504 [arXiv:2012.09389] [INSPIRE].

[45] O.H.E. Philcox, *Cosmology without window functions. II. Cubic estimators for the galaxy bispectrum*, *Phys. Rev. D* **104** (2021) 123529 [arXiv:2107.06287] [INSPIRE].

[46] F.-S. Kitaura et al., *The clustering of galaxies in the SDSS-III Baryon Oscillation Spectroscopic Survey: mock galaxy catalogues for the BOSS Final Data Release*, *Mon. Not. Roy. Astron. Soc.* **456** (2016) 4156 [arXiv:1509.06400] [INSPIRE].

[47] S.A. Rodríguez-Torres et al., *The clustering of galaxies in the SDSS-III Baryon Oscillation Spectroscopic Survey: modelling the clustering and halo occupation distribution of BOSS CMASS galaxies in the Final Data Release*, *Mon. Not. Roy. Astron. Soc.* **460** (2016) 1173 [arXiv:1509.06404] [INSPIRE].

[48] E. Aver, K.A. Olive and E.D. Skillman, *The effects of He I λ10830 on helium abundance determinations*, *JCAP* **07** (2015) 011 [arXiv:1503.08146] [INSPIRE].

[49] R.J. Cooke, M. Pettini and C.C. Steidel, *One Percent Determination of the Primordial Deuterium Abundance*, *Astrophys. J.* **855** (2018) 102 [arXiv:1710.11129] [INSPIRE].

[50] N. Schöneberg, J. Lesgourgues and D.C. Hooper, *The BAO+BBN take on the Hubble tension*, *JCAP* **10** (2019) 029 [arXiv:1907.11594] [INSPIRE].

[51] Planck collaboration, *Planck 2018 results. VI. Cosmological parameters*, *Astron. Astrophys.* **641** (2020) A6 [*Erratum ibid.* **652** (2021) C4] [arXiv:1807.06209] [INSPIRE].

[52] DESI collaboration, *DESI 2024 II: sample definitions, characteristics, and two-point clustering statistics*, *JCAP* **07** (2025) 017 [arXiv:2411.12020] [INSPIRE].

[53] A. Taruya, T. Nishimichi and S. Saito, *Baryon Acoustic Oscillations in 2D: Modeling Redshift-space Power Spectrum from Perturbation Theory*, *Phys. Rev. D* **82** (2010) 063522 [arXiv:1006.0699] [INSPIRE].

[54] F. Beutler et al., *The 6dF Galaxy Survey: Baryon Acoustic Oscillations and the Local Hubble Constant*, *Mon. Not. Roy. Astron. Soc.* **416** (2011) 3017 [arXiv:1106.3366] [INSPIRE].

[55] A.J. Ross et al., *The clustering of the SDSS DR7 main Galaxy sample — I. A 4 per cent distance measure at $z = 0.15$*, *Mon. Not. Roy. Astron. Soc.* **449** (2015) 835 [arXiv:1409.3242] [INSPIRE].

JCAP04(2026)030

[56] H. du Mas des Bourboux et al., *The Completed SDSS-IV Extended Baryon Oscillation Spectroscopic Survey: Baryon Acoustic Oscillations with Lyα Forests*, *Astrophys. J.* **901** (2020) 153 [arXiv:2007.08995] [INSPIRE].

[57] DES collaboration, *Dark Energy Survey Year 3 results: Cosmological constraints from galaxy clustering and weak lensing*, *Phys. Rev. D* **105** (2022) 023520 [arXiv:2105.13549] [INSPIRE].

[58] DES collaboration, *Dark Energy Survey Year 3 results: Constraints on extensions to ΛCDM with weak lensing and galaxy clustering*, *Phys. Rev. D* **107** (2023) 083504 [arXiv:2207.05766] [INSPIRE].

[59] DES collaboration, *Dark Energy Survey Year 3 results: Optimizing the lens sample in a combined galaxy clustering and galaxy-galaxy lensing analysis*, *Phys. Rev. D* **103** (2021) 043503 [arXiv:2011.03411] [INSPIRE].

[60] DES collaboration, *Dark Energy Survey year 3 results: covariance modelling and its impact on parameter estimation and quality of fit*, *Mon. Not. Roy. Astron. Soc.* **508** (2021) 3125 [arXiv:2012.08568] [INSPIRE].

[61] DES collaboration, *Dark Energy Survey Year 3 Results: Multi-Probe Modeling Strategy and Validation*, arXiv:2105.13548 [INSPIRE].

[62] A. Mead, S. Brieden, T. Tröster and C. Heymans, *HMCODE-2020: improved modelling of non-linear cosmological power spectra with baryonic feedback*, *Mon. Not. Roy. Astron. Soc.* **502** (2021) 1401 [arXiv:2009.01858] [INSPIRE].

[63] A. Spurio Mancini et al., *CosmoPower: emulating cosmological power spectra for accelerated Bayesian inference from next-generation surveys*, *Mon. Not. Roy. Astron. Soc.* **511** (2022) 1771 [arXiv:2106.03846] [INSPIRE].

[64] DESI collaboration, *DESI DR2 results. II. Measurements of baryon acoustic oscillations and cosmological constraints*, *Phys. Rev. D* **112** (2025) 083515 [arXiv:2503.14738] [INSPIRE].

[65] M. Tristram et al., *Cosmological parameters derived from the final Planck data release (PR4)*, *Astron. Astrophys.* **682** (2024) A37 [arXiv:2309.10034] [INSPIRE].

[66] DES collaboration, *The Dark Energy Survey Supernova Program: Cosmological Analysis and Systematic Uncertainties*, *Astrophys. J.* **975** (2024) 86 [arXiv:2401.02945] [INSPIRE].

[67] A. Chudaykin, M.M. Ivanov, O.H.E. Philcox and M. Simonović, *Nonlinear perturbation theory extension of the Boltzmann code CLASS*, *Phys. Rev. D* **102** (2020) 063533 [arXiv:2004.10607] [INSPIRE].

[68] A. Oddo et al., *Toward a robust inference method for the galaxy bispectrum: likelihood function and model selection*, *JCAP* **03** (2020) 056 [arXiv:1908.01774] [INSPIRE].

[69] A. Oddo et al., *Cosmological parameters from the likelihood analysis of the galaxy power spectrum and bispectrum in real space*, *JCAP* **11** (2021) 038 [arXiv:2108.03204] [INSPIRE].

[70] F. Rizzo et al., *The halo bispectrum multipoles in redshift space*, *JCAP* **01** (2023) 031 [arXiv:2204.13628] [INSPIRE].

[71] P. Carrilho et al., *Interacting dark energy from redshift-space galaxy clustering*, *JCAP* **10** (2021) 004 [arXiv:2106.13163] [INSPIRE].

[72] M. Tsedrik et al., *Interacting dark energy from the joint analysis of the power spectrum and bispectrum multipoles with the EFTofLSS*, *Mon. Not. Roy. Astron. Soc.* **520** (2023) 2611 [arXiv:2207.13011] [INSPIRE].

JCAP04(2026)030

[73] R. Scoccimarro, H.M.P. Couchman and J.A. Frieman, *The Bispectrum as a Signature of Gravitational Instability in Redshift-Space*, *Astrophys. J.* **517** (1999) 531 [astro-ph/9808305] [INSPIRE].

[74] P. McDonald and A. Roy, *Clustering of dark matter tracers: generalizing bias for the coming era of precision LSS*, *JCAP* **08** (2009) 020 [arXiv:0902.0991] [INSPIRE].

[75] V. Desjacques, D. Jeong and F. Schmidt, *Large-Scale Galaxy Bias*, *Phys. Rep.* **733** (2018) 1 [arXiv:1611.09787] [INSPIRE].

[76] A. Hall, *Cosmology from weak lensing alone and implications for the Hubble tension*, *Mon. Not. Roy. Astron. Soc.* **505** (2021) 4935 [arXiv:2104.12880] [INSPIRE].

[77] A. Reeves, P. Zhang and H. Zheng, *Debiasing inference in large-scale structure with non-flat volume measures*, arXiv:2507.20991 [INSPIRE].

[78] M.M. Ivanov et al., *Precision analysis of the redshift-space galaxy bispectrum*, *Phys. Rev. D* **105** (2022) 063512 [arXiv:2110.10161] [INSPIRE].

[79] S. Yuan et al., *The DESI one-percent survey: exploring the halo occupation distribution of luminous red galaxies and quasi-stellar objects with AbacusSummit*, *Mon. Not. Roy. Astron. Soc.* **530** (2024) 947 [arXiv:2306.06314] [INSPIRE].

[80] A. Rocher et al., *The DESI One-Percent survey: exploring the Halo Occupation Distribution of Emission Line Galaxies with AbacusSummit simulations*, *JCAP* **10** (2023) 016 [arXiv:2306.06319] [INSPIRE].

[81] A. Smith et al., *Generating mock galaxy catalogues for flux-limited samples like the DESI Bright Galaxy Survey*, *Mon. Not. Roy. Astron. Soc.* **532** (2024) 903 [arXiv:2312.08792] [INSPIRE].

[82] DESI collaboration, *DESI 2024 VII: cosmological constraints from the full-shape modeling of clustering measurements*, *JCAP* **07** (2025) 028 [arXiv:2411.12022] [INSPIRE].

[83] B. Stölzner et al., *KiDS-Legacy: Consistency of cosmic shear measurements and joint cosmological constraints with external probes*, *Astron. Astrophys.* **702** (2025) A169 [arXiv:2503.19442] [INSPIRE].

[84] M. Cortês and A.R. Liddle, *Interpreting DESI's evidence for evolving dark energy*, *JCAP* **12** (2024) 007 [arXiv:2404.08056] [INSPIRE].

[85] D. Shlivko and P.J. Steinhardt, *Assessing observational constraints on dark energy*, *Phys. Lett. B* **855** (2024) 138826 [arXiv:2405.03933] [INSPIRE].

[86] DESI collaboration, *DESI 2024: reconstructing dark energy using crossing statistics with DESI DR1 BAO data*, *JCAP* **10** (2024) 048 [arXiv:2405.04216] [INSPIRE].

[87] DESI collaboration, *DESI 2024: Constraints on physics-focused aspects of dark energy using DESI DR1 BAO data*, *Phys. Rev. D* **111** (2025) 023532 [arXiv:2405.13588] [INSPIRE].

[88] DESI collaboration, *Extended dark energy analysis using DESI DR2 BAO measurements*, *Phys. Rev. D* **112** (2025) 083511 [arXiv:2503.14743] [INSPIRE].

[89] DESI collaboration, *Dynamical dark energy in light of the DESI DR2 baryonic acoustic oscillations measurements*, *Nat. Astron.* **9** (2025) 1879 [*Erratum ibid.* **9** (2025) 1898] [arXiv:2504.06118] [INSPIRE].

[90] DESI collaboration, *DESI 2024 VI: cosmological constraints from the measurements of baryon acoustic oscillations*, *JCAP* **02** (2025) 021 [arXiv:2404.03002] [INSPIRE].

[91] Z. Lu, T. Simon and P. Zhang, *Preference for evolving dark energy in light of the galaxy bispectrum*, arXiv:2503.04602 [INSPIRE].

JCAP04(2026)030

[92] BOSS collaboration, *The clustering of galaxies in the completed SDSS-III Baryon Oscillation Spectroscopic Survey: cosmological analysis of the DR12 galaxy sample*, *Mon. Not. Roy. Astron. Soc.* **470** (2017) 2617 [arXiv:1607.03155] [INSPIRE].

[93] BOSS collaboration, *The clustering of galaxies in the completed SDSS-III Baryon Oscillation Spectroscopic Survey: Cosmological implications of the Fourier space wedges of the final sample*, *Mon. Not. Roy. Astron. Soc.* **467** (2017) 2085 [arXiv:1607.03143] [INSPIRE].

[94] BOSS collaboration, *The clustering of galaxies in the completed SDSS-III Baryon Oscillation Spectroscopic Survey: baryon acoustic oscillations in the Fourier space*, *Mon. Not. Roy. Astron. Soc.* **464** (2017) 3409 [arXiv:1607.03149] [INSPIRE].

[95] BOSS collaboration, *The clustering of galaxies in the completed SDSS-III Baryon Oscillation Spectroscopic Survey: cosmological implications of the configuration-space clustering wedges*, *Mon. Not. Roy. Astron. Soc.* **464** (2017) 1640 [arXiv:1607.03147] [INSPIRE].

[96] BOSS collaboration, *The clustering of galaxies in the completed SDSS-III Baryon Oscillation Spectroscopic Survey: On the measurement of growth rate using galaxy correlation functions*, *Mon. Not. Roy. Astron. Soc.* **469** (2017) 1369 [arXiv:1607.03148] [INSPIRE].

[97] DESI collaboration, *Frequentist Cosmological Constraints from Full-Shape Clustering Measurements in DESI DR1*, arXiv:2508.11811 [INSPIRE].

JCAP04(2026)030